anomalies which had appeared in the central parts of survey lines from F to H and from B to I each other. Similar tendency is noticed with those prospected results by north-south survey lines.

4-1-3 Distirubtion of MF

As the FE anomalies of this area are often associated with low AR anomalies, the MF anomalies of this area almost coincide to those of FE. In other words, distribution of FE more than 10 will nearly coincide to that of FE more than 10 %. But there are some parts where MF anomalies are formed without association with FE anomalies because of some local ultra low ARs less than 5 Ω -m. If such is taken into account, the MF anomaly is nothing but the FE anomaly. In this sense, description about the MF will be omitted here.

4-2 K Area: Assif Imider

4-2-1 AR Distribution

Apparent resistivity in this area showed a wide range of variation, from about 8 Ω -m at minimum to about 20,000 Ω -m at maximum. The AR values have been roughly divided into 3 classes; those below 200 Ω -m have been classified as low AR, those between 200 Ω -m to 1,000 Ω -m as intermediate AR, and those above 1,000 Ω -m as high AR. They have been compiled into AR profiles as shown by PLs. from II-5-1 to II-5-6, through which plan maps of AR distribution were prepared as shown by PLs. from II-6-1 to II-6-3. From these data, the features of AR distribution will be summarized as below;

(1) Similar patterns of AR distribution were obtained on all the survey lines. The intermediate - low AR zone was detected near survey station 8, the high AR zone was deliniated near the stations between 11 and 13, and the low AR zones on both sides of the survey line. Macroscopically, these AR zones are continuous in southwest from survey line No. 6 to survey line No. 9.

(2) The high AR zone above 1,000 Ω -m corresponds to dolomite, while the distribution of intermediate - low AR zone corresponds to that of andesite.

Based upon each of the profiles along the survey lines, detail explanation of AR distribution will be given as follows;

(1) A high AR zone was detected on survey lines No. 6 to No. 2, centering around survey stations 12-13, in a way to continue from the shallow to the deep zones in the ground vertically. Another high AR zone in the similar pattern of distribution to the former, was also detected near survey stations of 11 and 12 on the survey lines No. 8 - No. 9 continuously.

(2) On the survey lines No. 6 - No. 2, low AR zones were detected on both sides of the high AR stated in (1), in a way of putting the high AR in between and continuously from the shallow to the deep parts of the ground. These high AR and low AR were detected in the assumable zones of dolomite distribution in the shallow ground and andesite distribution in the deep ground. Moreover, the high AR was detected at the mountain of topography and the low AR at the valley, and in accordance to the extension of these topographic mountain and valley in southwesterly, these high and low ARs are extended in the direction of southwest.

(3) A high AR zone was detected near stations 5 - 6 over the survey lines No. 6 - No. 9 continuously in the southwest direction, which appeared on the northwest side of the survey lines, continuing from the shallow to the deep parts in the ground.

(4) High AR zones were detected in the southeastern side of from around stations 17 - 18, on the survey lines No. 6 - No. 2, and in the southeastern side of around station 12 on the survey line No. 1, appearing from shallow to deep parts in the ground. The high AR stated above in (3) and this high AR nearly correspond to the distribution of dolomite on the surface.

(5) The intermediate AR zone appeared nearly in the centers of all the lines surveyed, from shallow to deep parts in the ground. But on the survey lines No. 6 - No. 4, the intermediate AR can hardly be taken as a significant zone, because the zones of high AR and low AR are swollen in the central parts of the survey lines. The intermediate zone was detected cumulatively around the central parts of the survey lines over No. 2 - No. 9, and small patches of low AR were detected scatteredly in the distribution of intermediate AR. These intermediate - low ARs, especially those over the survey lines No. 2 - No. 9, correspond to the distribution of andesite exposed on the surface, near survey station 8.

4-2-2 FE Distribution

The FE values in this area showed from less than 1 % to 15 %. They have been roughly divided into 4 classes; those less than 2 % have been classified as background, those between 2 % and 3 % as weak anomaly, those between 3 % to 5 % as intermediate anomaly, and those above 5 % as strong anomaly. These data were compiled into profiles along the survey lines, through which plan maps of FE distribution were prepared as PLs. from II-6-4 to II-6-6. Based upon these drawings, distribution of the detected anomalies will be explained as follows:

(1) A strong FE anomaly containing FE values more than 8 % and ranging from shallow to deep parts of the ground was detected near stations 11 - 18 on the survey line No. 6, around stations 11 - 16 on the survey line No. 4, and around stations 11 - 14 on the survey line No. 2. This strong FE anomaly continues from the survey line No. 6 to line No. 2 with similar patterns, accompanying with the strong AR stated in (1) of 4-2-1.

(2) The survey line No. 1 is the line crossing over the Assif Imider ore deposit, on which the FE anomaly derived by the known ore deposit was detected. That is to say, weak and intermediate anomalies were detected with local strong anomaly in a wide area, centering around station 8 on the survey line No. 1 and stretching from the shallow part near stations 6 - 11 towards the deep part below stations near 4 - 12.

The anomalies by the known ore body continue to the direction of southwest towards the survey lines No. 8 and No. 9. On the survey line No. 8, the weak anomaly was scarcely detected, but intermediate was detected ranging from the shallow part near stations 5 - 9 to the deep part below stations 3 - 11 in the ground. A local strong anomaly was detected in the shallow ground nearly below station 8. On the survey line No. 9 the weak and intermediate anomalies were detected in the deeper parts than what were detected on the survey lines No. 1 and 8.

To examine the continuity of anomalies in the northeastern direction, small scaled anomalies of low and intermediate were detected on the survey line No. 2, spreading from the shallow ground below about stations 7 - 8 to the direction of northwest. Small scaled weak and intermediate anomalies

were detected in the deep ground nearly below stations 4 - 5 on the survey line No. 4. Small scaled weak anomaly was also detected in the deeper ground nearly below stations 4 - 6 on the survey line No. 6.

Thus, the anomalies continue to the northeast too, but compared to the southwest, the anomalies become smaller and exist deeper.

The anomalies inferable to the known ore deposit and its extension were detected in the possible areas of the andesite to be distributed.

(3) Weak and intermediate anomalies were detected near stations 15 - 16 on the survey line No. 2 and near station 8 on the survey line No. 8. They were so detected as to correspond to the exposures of andesite on the surface, although their distribution could not be fully cleared, as they were located at the terminals of the survey lines.

4-2-3 Distribution of MF

As MF is a function of FE, the detailed explanation on each survey line will be omitted here. To say about the general aspect, the distribution of MF in this area nearly coincides to that of FE due to the fair correlation between the distributions of FE anomaly and low and intermediate ARs. The known ore deposit of Assif Imider is included in an area deliniated by equivalent curves of FE more than 10. This equivalent line of MF 10 surrounds in the shallow ground but does not reach deeper. A strong anomaly exceeding MF 100 spreads centering around the eastern measuring station 13 of the survey lines No. 6 - No. 2.

Chapter 5 Interpretation of Underground Structure by Simulation

The attached plates II-8-1 and II-8-2 are the panel diagrams, composed of profiles on which stronger FE response bodies inferable from simulation have been drown, which have been so arranged as to aid for easy understanding of interrelations of the survey lines each other. Comparisons between the measured values from IP survey and the calculated values obtained through simulation are shown by Figs. from II-5-1 to II-5-4.

5-1 Talat-n-Sous Area

The representative FE indications in this area are, as stated in 4-1, the large scaled FE anomaly which spreads in the central and northern parts of the survey lines B - H, and nother FE anomaly spreading in the southern parts of the survey lines I - N. Estimation of underground structure by simulation were tried on the ranges of stations from 9 to 21 on the survey line G and from O to 12 on the survey line K by selecting these two lines as the representatives of these FE anomalies.

5-1-1 G Line, Stations 9 - 21 (cf. Figs. II-5-1a & b)

The topographic adjustment was not made on this line, as the topographic influence was thought to be out of consideration. By assuming a horizontal slab in the surface formation of sandstone and siltstone and by giving FE 5 % and AR 100 - 300 Ω -m, and by assuming the bodies from prismatic to massive and by giving FE 7 % and AR 300 Ω -m in the deep ground, the patterns of IP indications through theoretical calculation showed close approximation to that of by the measured values. The structural features in the ground inferable from the results are stated as follows:

(1) The thickness of sandstone and siltstone are estimated about 50 m - 100 m around survey stations 13 - 16, which is thicknened on both sides and is estimated to be thickneed about 200 - 300 m finally. Near survey station 20 in the north side, the thickness of sandstone and silstone is estimated to be thinned again, and moreover, an FE response body in a slab is inferred in the shallow ground near the station 13 - 17.

(2) A rock body of high AR can be estimated beneath the sandstone and siltstone. Rock bodies from prismatic to massive is inferred on both sides of the high AR rock body.

5-1-2 K Line, Stations O - 12 (cf. Figs. II-5-2a & b)

Simulation was made directly on the results of field measurements without giving topographic adjustment as this survey line was felt unnecessary to be adjusted. The inferred structure through the simulation, showed an approximation to the geological profile obtained through the surface geological informations. In other words, it showed a structure of bedded slabs inclined to the south as a whole. The structural bodies estimated from the surface distribution are shown by 100 - 300 Ω -m for the sandstone and siltstone, 400 Ω -m for the conglomerate, and 500 - 1,000 Ω -m for the dolomite.

The major characteristics of the inferred structural bodies is that an inclined slab with low AR and high FE is estimated to exist between the structural bodies corresponding to the conglomerate (3) and the dolomite (1).

The following features may be said about the inferred underground structure in addition to that stated above:

(1) The sandstone and siltstone increase the thickness from around station 6 with southward dip.

(2) Dolomite in Basal Series is considered to underlie the sandstone and siltstone with constant thickness (within 50 m), dipping to the south.

(3) A rock body of low AR can be inferred, underlying unconformably the dolomite of Basal Series. This rock body with low AR is estimated to be concealed in the depth of about 100 - 200 m.

(4) The PIII conglomerate is estimated to lie below the dolomite of Basal Series and the low AR rock body above mentioned from the surface around stations 10 and 11, increasing its thickness towards south.

(5) The PII-III rhyolitic tuffs are considered to be developed under the conglomerate above mentioned, of which depth is about 100 m below the surface near station 10, and about 200 m below the surface near station 7.

(6) A massive response body is inferred in the low AR rock body which can be considered to exist in the deep ground near stations 3 - 6.

(7) A small scaled slabby response body is also inferred in the sandstone and siltstone in the shallow ground near stations 5 and 6.

5-2 Assif Imider Area

The IP indications in this area are characterized by a small FE anomaly detected around the andesite exposures and nearby mineralized zone in the southwestern part and another FE anomaly of larger scale corresponding to the distribution of andesite in deep ground. Simulation was made on the range between survey stations 2 and 14 on survey line No. 1 as a representative of these anomalies. It was also made on between stations 8 and 20 on the survey line No. 6, as to be representative of the anomaly covering those formations from the andesite to the dolomite, conglomerate, sandstone, and shale of Basal Series, observed in the northeastern part.

5-2-1 Line No. 1, Stations 2 - 14 (cf. Figs. II-5-3a & b)

Topographic adjustment was given to this line first of all owing to the steep topography along this survey line. In making the topographic adjustment, the adjustment factor is calculated on two dimensional model by electronic computor, and then by dividing the measured value by the adjustment factor, distribution map of the adjusted AR is obtained. Based on this distribution map of adjusted AR, the simulation will be performed by electronic computor. The followings are the features of inferred underground structure:

(1) The dolomite showing high AR between 2,000 and 4,000 Ω -m is exposed on the surface, increasing its thickness to the both sides of survey lines.

(2) The andesite exposed near the center of the survey line shows AR of 300 Ω -m and is distributed throughout the ground.

(3) A small scaled slab with 300 Ω -m AR and 7 % FE is inferred in the andesite of the shallow ground. This may correspond to the strongly altered part in the andesite.

(4) A large inclined slab is inferred in the deep part of the andesite with AR of 300 - 500 Ω -m and 8 % FE. This response body is considered to have the similar electric properties with the small scale slab corresponding to the mineralized part of the andesite stated in (3).

5-2-2 Line No. 6, Stations 8 - 20 (cf. Figs. II-5-4a & b)

Topographic adjustment was made to this survey line too, because of steep topography similarly to the survey line No. 1 for the distribution of AR. Distribution of AR and FE along this line resembles to the pattern of anomaly detected on Basal Series in the south side of the survey lines during the survey of the second year phase in Alous Area. By assuming a horizontal slab corresponding to the layers of conglomerate, sandstone, and shale distributed near the surface between stations 12 and 20, and by giving FE of 9.5 %, the calculated results showed a close approximation. From this, the inferred underground structure will be mentioned as follows:

(1) The dolomite and conglomerate are distributed almost horizontally.

(2) The dolomite shows high AR of 3,000 Ω -m.

(3) A horizontal slab with AR of 100 Ω -m and FE of 9.5 % is inferred in the partly exposed conglomerate, sandstone, and shale of Basal Series. Considering the surface geological showings, it is considered to indicate pyrite contained in the formation.

(4) But it has to be kept in mind, that sometimes an FE response body in the deep ground will not be detected, being masked by a strong FE response body near the surface in case it is as strong as 9.5 % FE due to strong influence from the electrodes on the surface, as is usually the case in electrical prospecting.

Fig II-5-1a FIELD RESULTS ON LINE.G
(TALAT-N-SOUS)

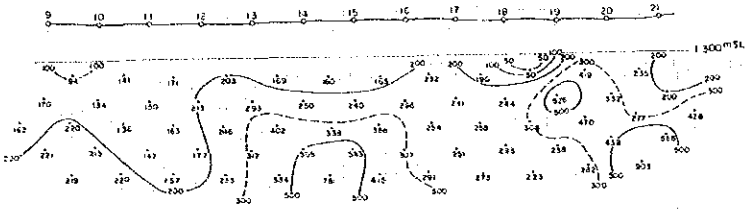

MEASURED APPARENT RESISTIVITY

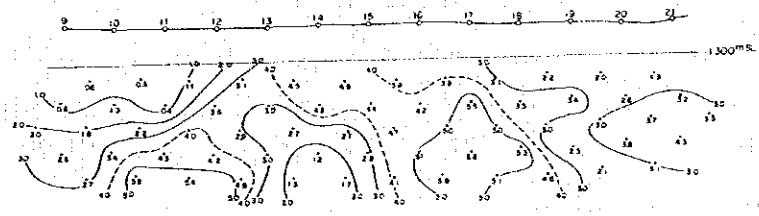

MEASURED FREQUENCY EFFECT

Fig II-5-1b RESULTS OF COMPUTOR MODELING
ON LINE.G (TALAT-N-SOUS)

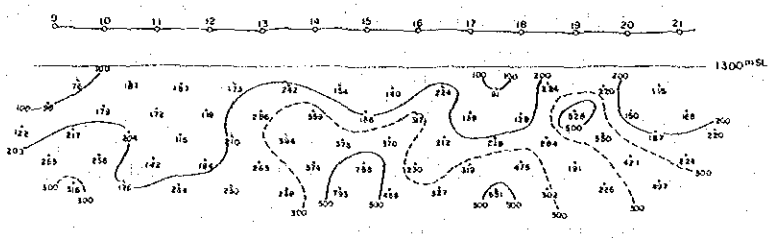

CALCULATED APPARENT
RESISTIVITY

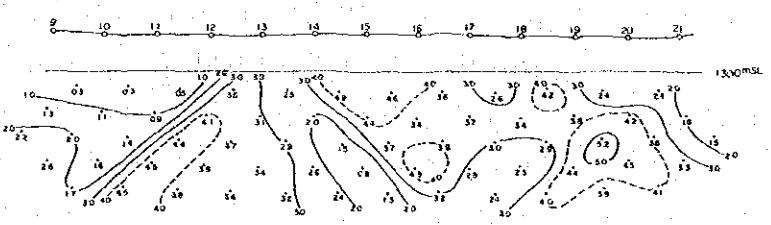

CALCULATED FREQUENCY
EFFECT

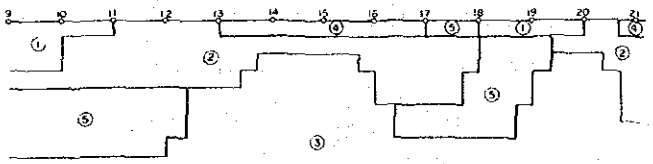

SIMULATED MODEL

NO	Resistivity	F.E
①	100 Ωm	1.0 %
②	350	1.0
③	1,000	1.0
④	100	5.0
⑤	300	7.0

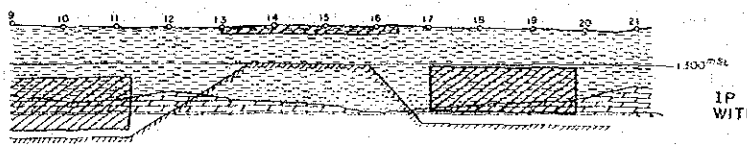

IP RESPONSE BODIES ASSUMED
WITH THE GEOLOGY

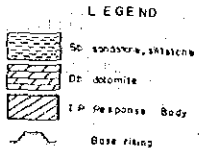

Fig II-5-2a FIELD RESULTS ON LINE.K
(TALAT-N-SOUS)

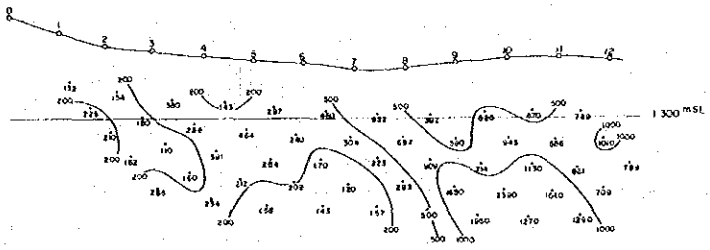

MEASURED APPARENT RESISTIVITY

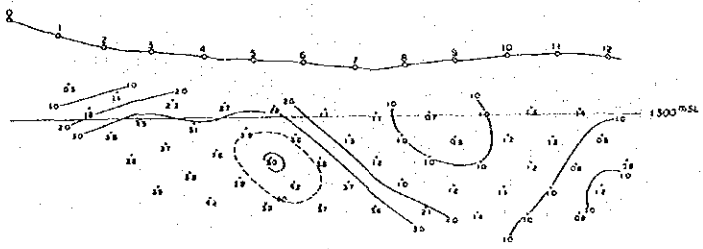

MEASURED FREQUENCY EFFECT

Fig II-5-2b RESULTS OF COMPUTOR MODELING ON LINE K (TALAT-N-SOUS)

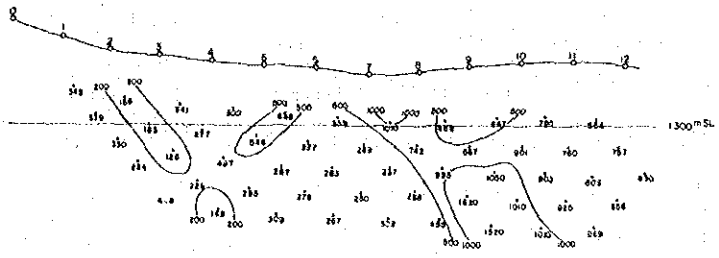

CALCULATED APPARENT RESISTIVITY

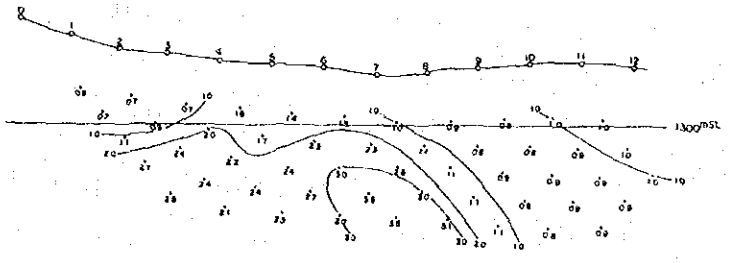

CALCULATED FREQUENCY EFFECT

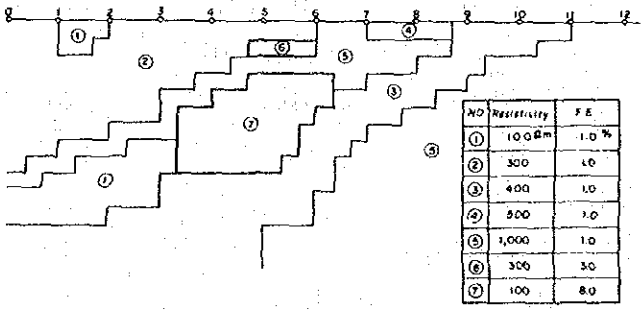

NO	Resistivity	F.E.
①	100Ωm	1.0 %
②	300	1.0
③	400	1.0
④	500	1.0
⑤	1,000	1.0
⑥	300	3.0
⑦	100	8.0

SIMULATED MODEL

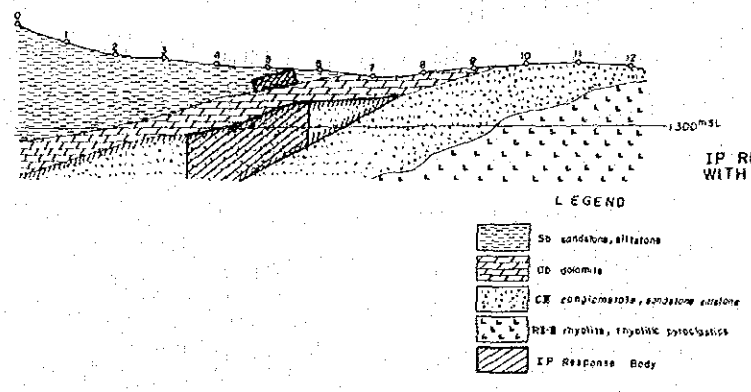

IP RESPONSE BODIES ASSUMED WITH THE GEOLOGY

Fig II-5-3a FIELD RESULTS ON LINE NO.1 (ASSIF IMIDER)

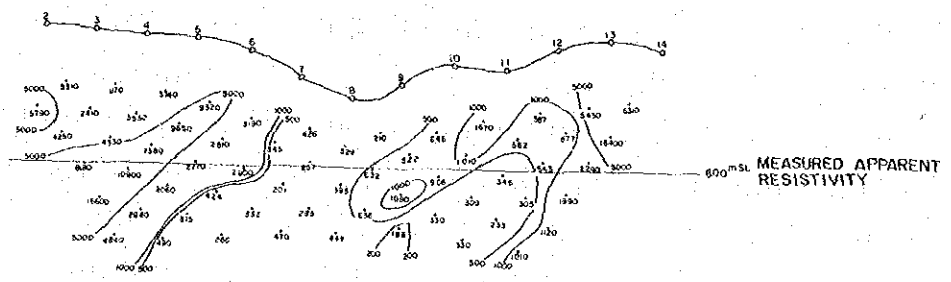

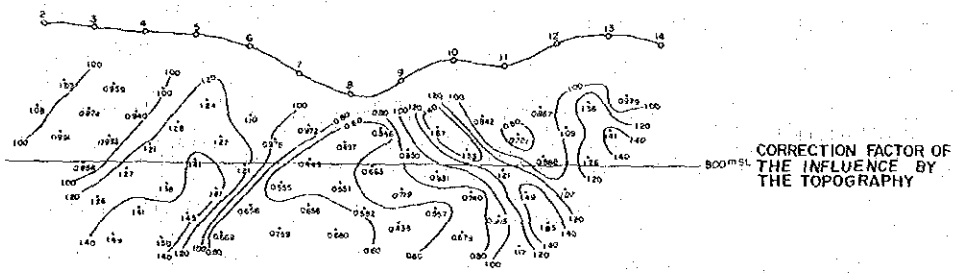

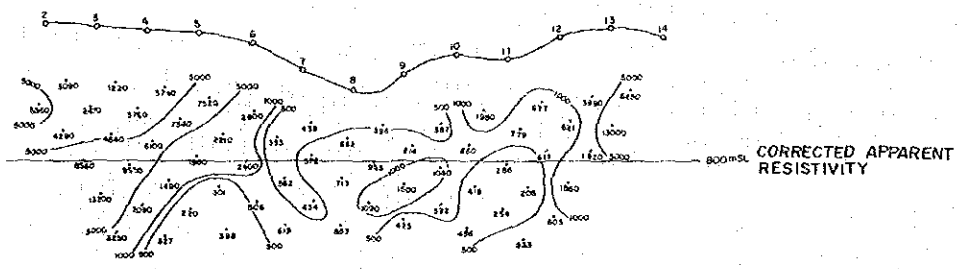

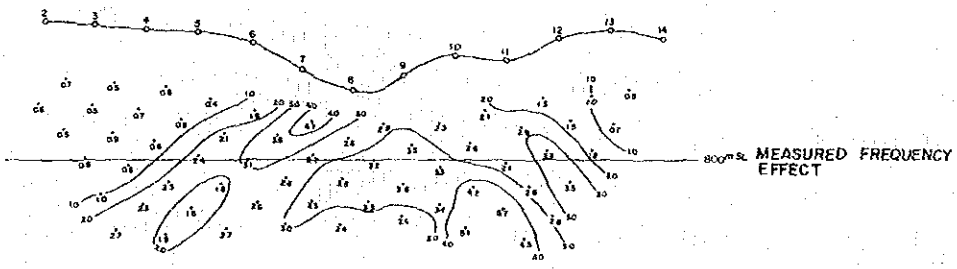

Fig II-5-3b RESULTS OF COMPUTOR MODELING ON LINE NO.1 (ASSIF IMIDER)

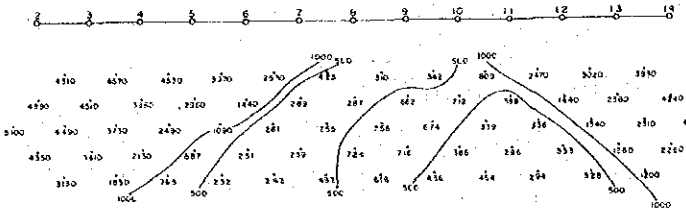

CALCULATED APPARENT RESISTIVITY

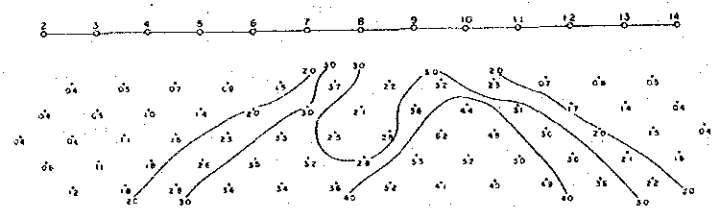

CALCULATED FREQUENCY EFFECT

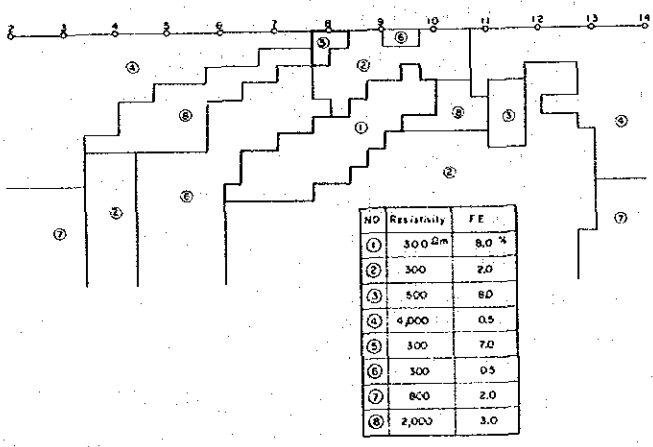

NO	Resistivity	F E
①	300 Ωm	8.0 %
②	300	2.0
③	500	8.0
④	4,000	0.5
⑤	300	7.0
⑥	300	0.5
⑦	800	2.0
⑧	2,000	3.0

SIMULATED MODEL

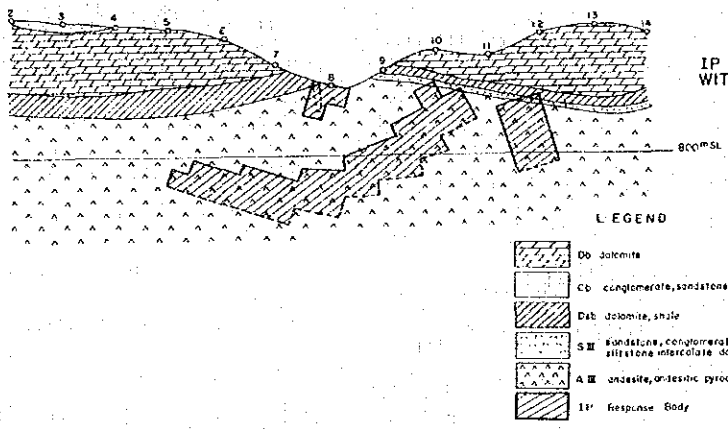

IP RESPONSE BODIES ASSUMED WITH THE GEOLOGY

Fig II-5-4a FIELD RESULTS ON LINE NO.6 (ASSIF IMIDER)

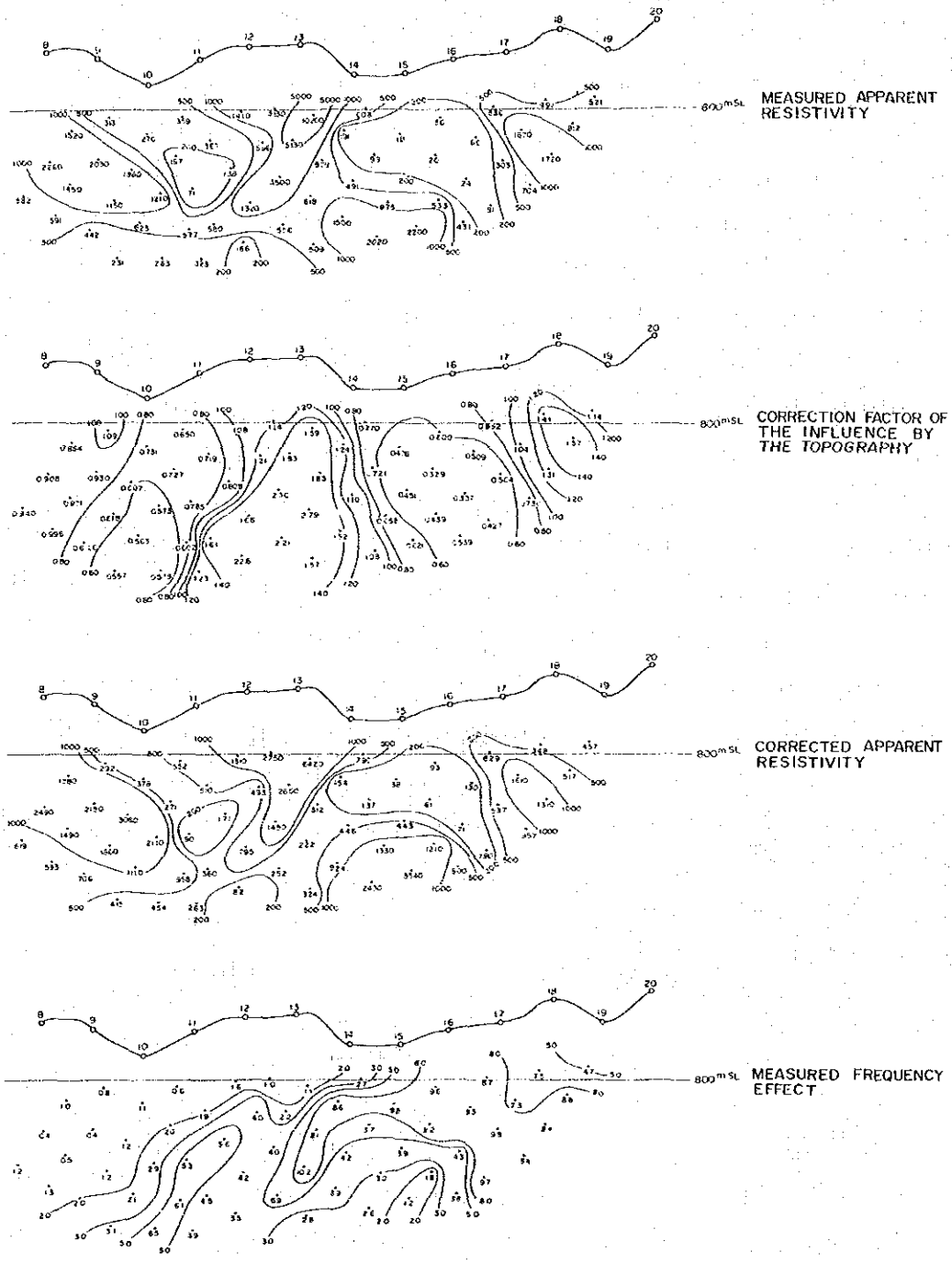

Fig II-5-4b RESULTS OF COMPUTOR MODELING ON LINE NO.6 (ASSIF IMIDER)

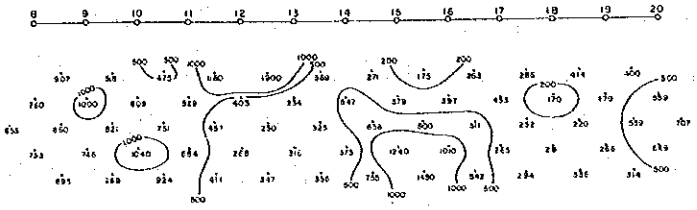

CALCULATED APPARENT RESISTIVITY

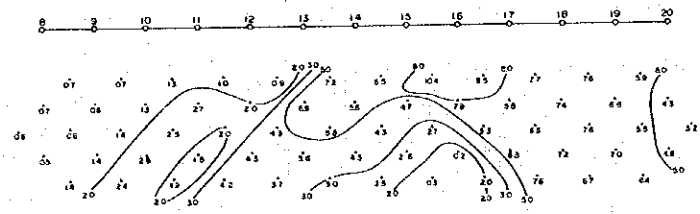

CALCULATED FREQUENCY EFFECT

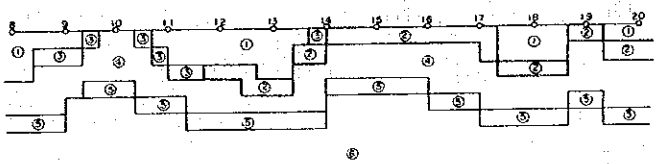

SIMULATED MODEL I

NO	Resistivity	FE	Geology
①	3,000 Ω-m	0.5 %	Db
②	100	9.5	Cb with pyrite
③	100	1.0	Cb
④	800	1.0	Db
⑤	300	1.0	Dsb, SH
⑥	800	1.0	AH

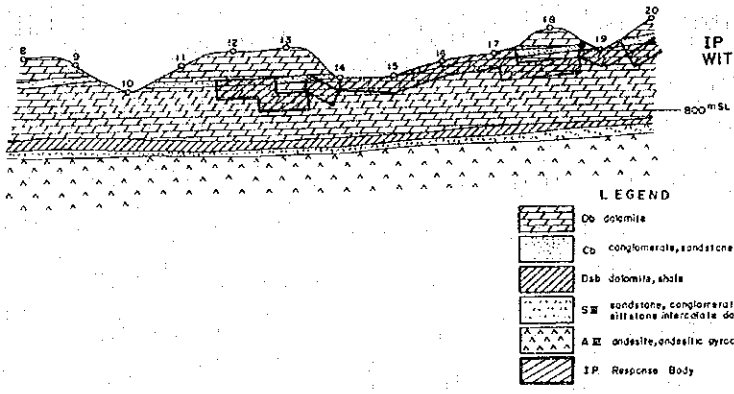

IP RESPONSE BODIES ASSUMED WITH THE GEOLOGY

Chapter 6 Underground Structure Inferred by IP Survey

6-1 Talat-n-Sous Area (cf. PL. II-8-1, Fig. II-6-1)

The underground structure inferred by the IP indications in this area will be summarized as follows:

(1) The dolomite of Lower Calcareous Series distributed in the northwestern part of the area shows high AR but background values of FE. Judging from such IP indication, the dolomite of Lower Calcareous Series shows a thin layered structure in the southwest, while in the northeast, shows a thick layered structure towards north, being bordered by the fault (or fractured zone) which will be stated in (2).

(2) Low AR zone, being emplaced near the contact between the dolomite of Lower Calcareous Series and the sandstone and siltstone of Basal Series, continues from the survey line B till Q. From the continuity of this low AR zone, an existence of a fault or fractured zone is assumed. It is so distributed as to continue eastwesterly between the survey lines B and D at around stations 20 and 21, but from around stations 20 and 21 on the survey line D it is switched to continue towards stations 26 and 27 on the survey line G, in a direction of NE-SW system.

(3) A large FE anomaly was detected which continues between the survey lines B and F at the central parts of the lines. The FE response body (Rt-2) to have caused this anomaly seems to be slabby and to continue to the line Q with repeated gentle undulation in east-west direction, and is estimated to exist in the sandstone and siltstone. According to the informations of geological survey, however, as the eastwesterly folding structure can hardly be recognized, there is strong possibility that the response body may exist as some layers in the different horizons. The FE response body (Rt-2) is considered to indicate the sulphides such as pyrite and others contained in the sandstone and siltstone of Basal Series, which has been made clear by the boring practiced during the current survey in Alous Area.

(4) A large scaled FE anomaly was detected to continue from the survey line G to H at the central parts of the survey lines. The response body (Rt-1) possibly derived the anomaly is estimated in a slabby form, existing in the sandstone. This FE response body is near the surface around the survey line H and continues till to the vicinity of the survey line G, being inclined to the west. This FE response body, as stated in (3), is estimated to indicate the sulphides such as pyrite in Basal Series similarly to the FE response body (Rt-2). As there is scarcely none of the eastwesterly folding recognized field geologically, the FE response bodies (Rt-1) and (Rt-2) are estimated with the strongest possibility to exist in layers in the different formations.

(5) A doming up of a layer with high AR, probably derived by the dolomite, is inferred near stations 17 - 10 around the survey lines G - S, and FE response body (Rt-3) in massive - prismatic form is inferred on both sides of the doming up. At present moment, it is difficult to explain geologically about the hidden existence of FE response body to exist on both sides of high AR layer.

(6) The igneous rocks of PII-PIII formations and the PIII conglomerates are widely distributed on the surface in the east from the survey line Q. No prominent FE indications were detected within the distribution of these formations, but a few groups of very faint FE about 1 % were recognized within the distribution of FE estimated as background. The followings will be inferred from these facts.

1) The mineralized zone found in a trench near station 18 of the survey line J contains very little amount of sulphides. But it is considered that the contents are scanty and the mineralized zone is thin, because no FE anomaly has ever been detected. Nevertheless, as a group of FE values about 1 %, which are considered to indicate the extension of the mineralized zone, are recognized near the stations 15 - 17 of the survey line Q, some downward extension may be anticipated.

2) Mineral indications have been recognized through geological survey along the surface of unconformity between Basal Series and PII-PIII formation in addition to the one stated above in (1), but non of FE anomaly

has been detected to reflect them. That the minerals on the surface have been altered into the secondary minerals such as oxides and/or carbonates, and that the thickness of the mineralized zone is very thin, will be counted for the reason.

(7) Around stations 4 and 5 of the survey lines from K to N, similar patterns of IP indications were detected continuously. The results of simulation, as stated in Chapter 5, indicated an upper response body in a small scaled slab existing in the sandstone and siltstone, and another lower FE response body of an inclined slab (Rt-5) with low AR and strong FE in the deeper ground. The upper one is considered to indicate pyrite contained in the sandstone and siltstone. The lower response body is the one to be extended for more than 100 m in a direction of N - S, and is to be developed deeper. Several cases will be possible to interpret such response body in the lower part of Basal Series from the geological informations in this area, for instance:

1) The case of sulphide concentration in the faults or fractured zones which are hidden in the conglomerate (or andesite) of PIII formation.

2) The case of iron oxides in the andesite as recognized by the results of diamond boring in Alous Area.

3) The case of existing of sulphides or copper mineralization in the hidden distribution of conglomerates of Basal Series.

Among these cases, the hidden existence of the faults or fractured zones is necessary to be assumed for the case 1). For the case 2), doming up of andesite is necessary to be considered along with the thinning of dolomite and conglomerate below the survey lines K - N in spite of their wide distribution on the surface, and such a negative factor has to be considered too, that none of FE anomaly has been detected over the andesite exposed on the surface. The case 3) seems more possible in view of such affirmative factors that, (A) the PII conglomerate usually does not contain sulphides but the conglomerate of Basal Series is known to contain the sulphides, and there is distributed the conglomerate of Basal Series around the Amdouz Mine striking nearly in E - W system, and its continuity up to the surveyed area may possibly expected.

6-2 Assif Imider Area (cf. PL. II-8-2, Fig. II-6-2)

Followings are the underground structure inferred from the IP indications in this area:

(1) A small scaled slab corresponding to the known ore body was inferred in the shallow ground as the results of simulation tried on the IP indications detected over the known ore deposit centering around station 8 of the survey line No. 1. Another response body in a larger scaled inclined slab was also inferred to exist below the upper one. The deeper slab resembles in its electrical properties to the upper slab which corresponds to the ore deposit. But the lack of downward persistence has been proved by the boring formerly drilled. Moreover, scarcity of quantity of useful minerals contained around the larger FE response body in the andesite has also been disclosed by the results of boring drilled in Alous Area in the present year phase. Judging from these facts, the inclined slab inferred in this area may be interpreted in two ways; the one is the case when, in spite of the less amount of useful minerals, it indicates widely dispersed hematite (specularite) and others, which are FE responsible, in the andesite in the lower part of the ore deposit, and the other is the case of dissemination of pyrite and copper minerals.

The inferred structure as above (Ra-1) near the known ore deposit is shallowest on the survey line No. 8 in the south and continues to the line No. 9. While in the north, a small scaled slab is inferred in shallow ground, corresponding to the ore deposit and being extended to the line No. 2, but the larger slab below the known ore deposit was not detected in the north from the survey line No. 2, either because of its extinction or to its deeper existence.

(2) A strong anomaly in association with high AR was detected near station 13 spreading from the shallow to deep ground between the survey lines No. 6 and No. 2 in the north, and an IP indication of low AR less than 100 Ω-m was also detected continuously in a way to put the high in between.

This IP indication obtained from the measured values showed a close approximation to what was calculated by simulation, which was done by giving the values of high AR and low FE to the dolomite, by assuming a horizontal slab to the lower seated layers of conglomerate, sandstone, and

further by considering the topography (the dolomite lies in a thick layer near station 13, and its east and west sides are deeply eroded into steep valleys, where the lower seated conglomerate, sandstone, and siltstone are exposed out on the side slopes).

Judged from above, the conglomerate, sandstone, and shale are considered to contain much amount of pyrite with horizontal structure, which coincides to the surface geological showings.

(3) In the west of the survey lines No. 1 and No. 2, the conglomerate, sandstone, and shale are exposed widely, showing high AR and low FE. But the same formation observed in the northeast of the area shows low AR and high FE as stated in (2), and the electrical properties differ between the two. This may be attributed to the pyrite content in quite a quantity in the said formation of the northeast of the surveyed area, as has been cleared by geological survey.

(4) A weak FE anomaly has been detected near stations 15 and 16 on the survey line No. 2 and on the eastern terminal of the line No. 8 As the FE response body for this anomaly, a small sclaed slab can be inferred in the Shallow part of the exposed neighbouring formation consisting of andesite, sandstone, siltstone, and conglomerate. This may possibly be attributed to the content of non-useful minerals like pyrite in the andesite, or in the sandstone, siltstone, and conglomerate, in this area.

Fig II-6-1 GENERALIZED MAP OF IP SURVEY IN TALAT-N-SOUS

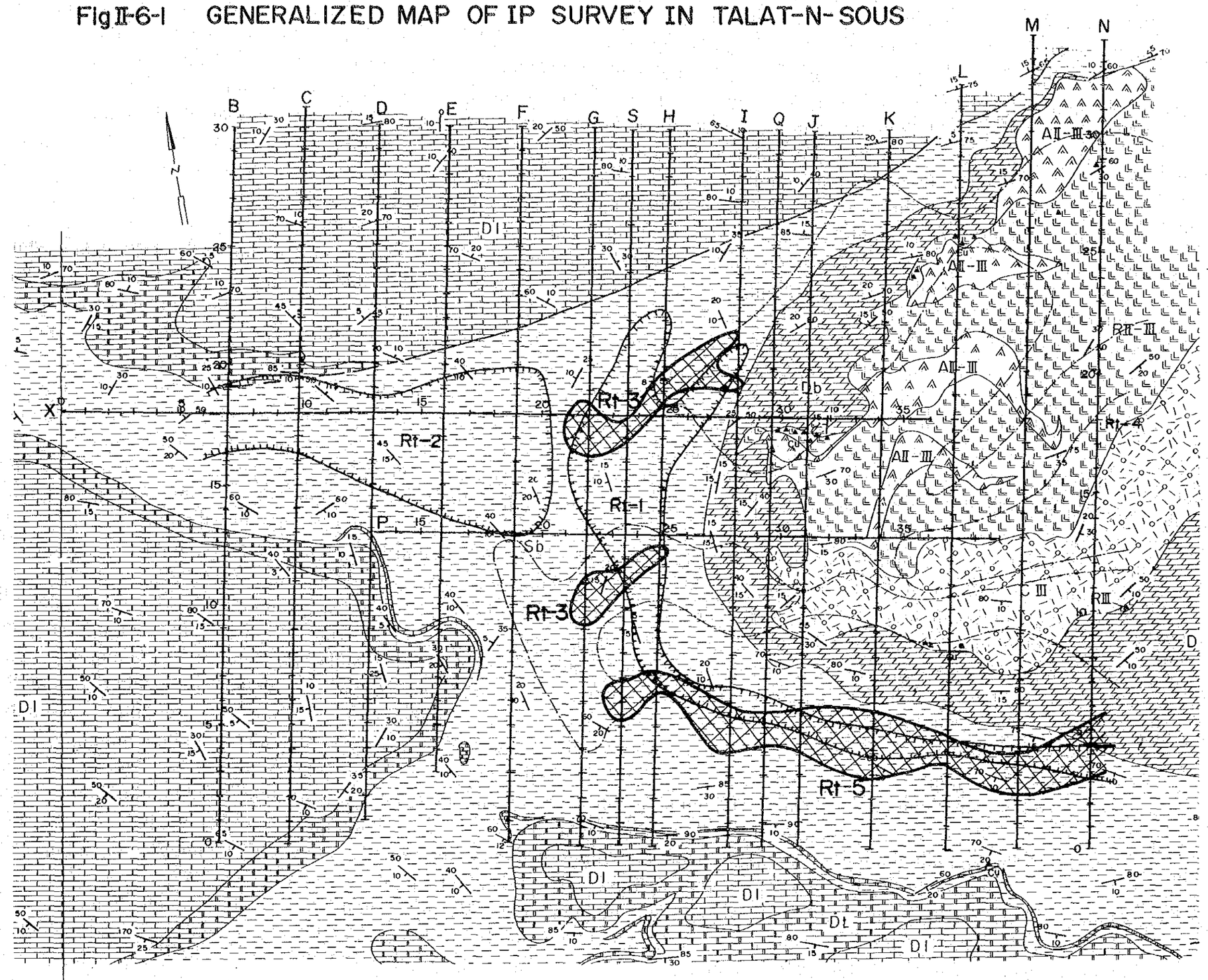

Fig II-6-2 GENERALIZED MAP OF IP SURVEY IN ASSIF IMIDER

Scale 1: 15,000

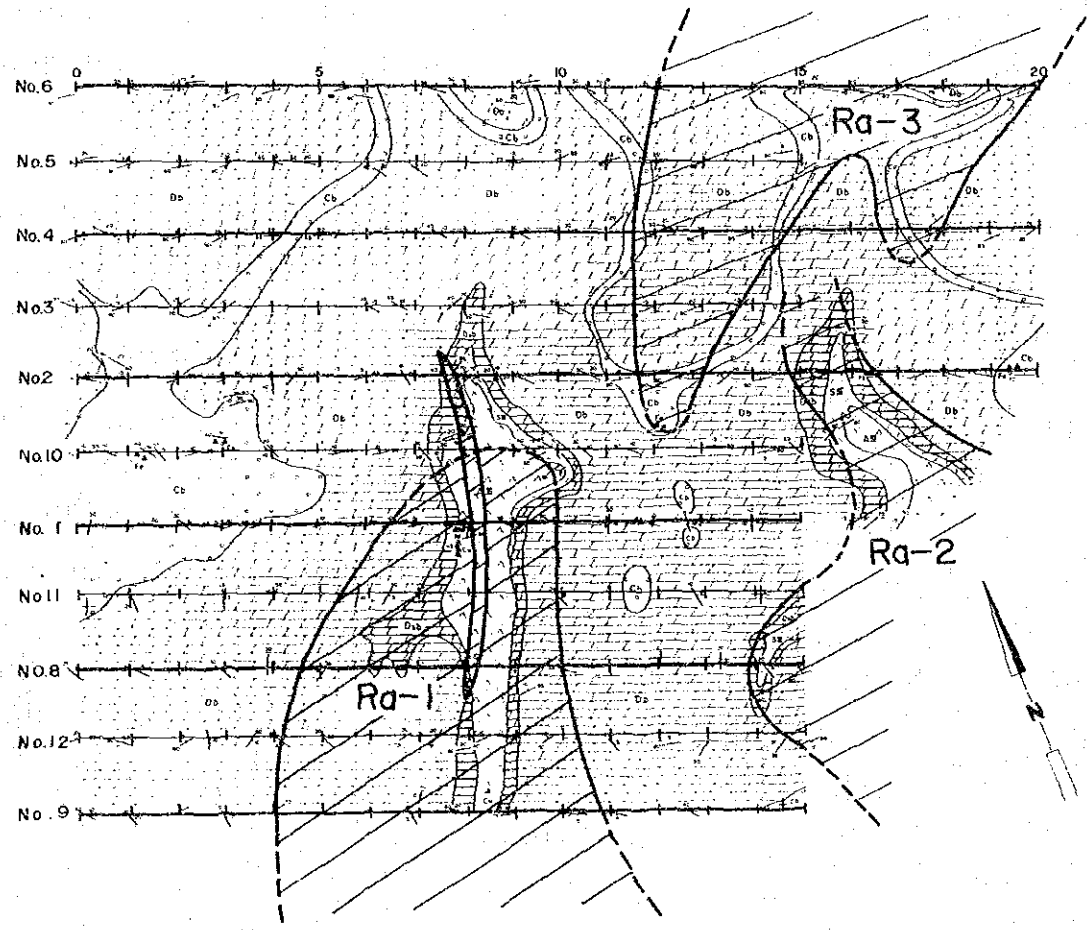

Chapter 7 Comparison between Geophysical Survey (IP method) and Boring in the Second Year Phase

Based upon the results of the geophysical survey by IP method in the second year phase, diamond boring was performed at around station 62 of the survey line E. The results of the IP survey and laboratory measurement of the drill cores are shown by Fig. II-7-1 just for comparison. Referring to the measured values of AR and FE in laboratory, simulation was made by electronic computor, of which results are shown by Fig. II-7-2.

Distinct characteristics of the laboratory measurement of drill cores are that the sandstone in the alternation of sandstone, shale and siltstone near the surface showed strong FE response of about 25 % and 5 %, and the andesite also showed itself as strong response body as from 2 % to 20 %. Pyrite is contained in the sandstone and hematite (specularite) in the andesite. Tamjout dolomite showed the response entirely below 1 %.

Taking into account of the data of laboratory measurement and geological informations obtained through surface geological survey and examination of the drill cores, models were given for simulation by electronic computor to make the calculated values approximated to the measured values. As is often the case that the detected stronger FE by IP survey does not response to the useful minerals, the response body detected in Alous on the survey line E is considered to reflect the existence of pyrite and hematite (specularite), as has been confirmed by the boring.

The results of data analysis in the second year phase are shown by Fig. II-6-4, Alous Line E in the report of the second year phase. The structure shown by the report has shown rectangular and prismatic shapes with strong FE of 10 %, existing in the shallow and deep ground centering around survey station 62. The simulation models in which the results of laboratory measurement of drill cores are taken into accoutn, is such that the strong FE response bodies have been added in the formation of sandstone, conglomerate, and shale as well as in the layter of andesite, showing an inclined layered structure. Compared with the analytical model, the both coincides in indicating the existence of massive FE response bodies in the shallow and deep ground centering around survey station 62, by which they may be treated equal macroscopically. But precisely speaking, there is slight difference

in the shallow structure near survey stations of 58 and 66.

In the survey of the second year phase, the massive response body was attributed to have been derived by the sulphide dissemination and alteration in the andesite near the boundary between the andesite and Basal Series, and/or underground water containing electrolyte. But the existence of copper sulphide minerals and others have been denied by the results of the boring, and it has come to be interpreted that selective concentration of pyrite impregnation in the sandstone and siltstone, and sulphides and oxides of iron in the andesite had caused to have been detected as a large scaled anomaly. Although the reason of selective local accumulation of iron minerals has not been solved by the survey yet, it is hoped that the mechanism of such occurrence will be solved some day and the result will serve for a key in the future prospecting for useful minerals.

Fig II-7-1 FIELD RESULTS ON LINE. E (ALOUS) & LABOLATORY MEASUREMENT ON D.H--No.1

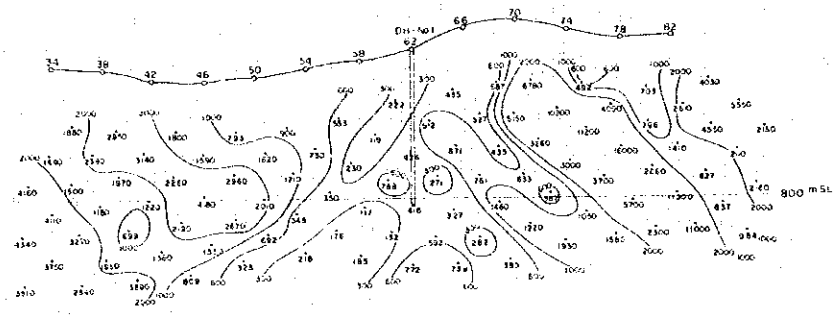

MEASURED APPARENT RESISTIVITY

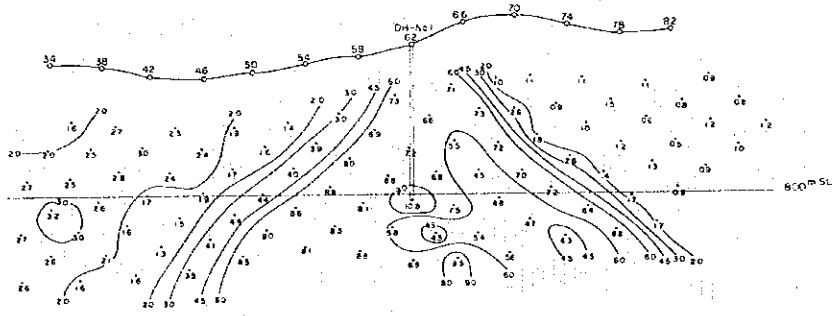

MEASURED FREQUENCY EFFECT

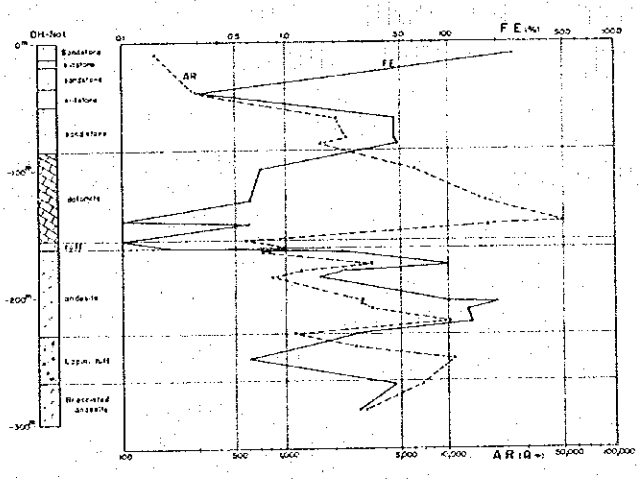

AR and FE LABOLATORY MEASUREMENT (DH-No.1)

Fig Ⅱ-7-2 RESULTS OF COMPUTOR MODELING ON LINE E (ALOUS)

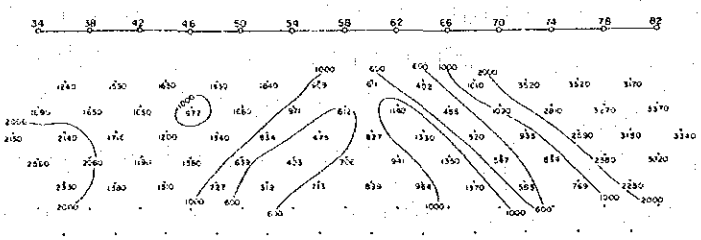

CALCULATED APPARENT RESISTIVITY

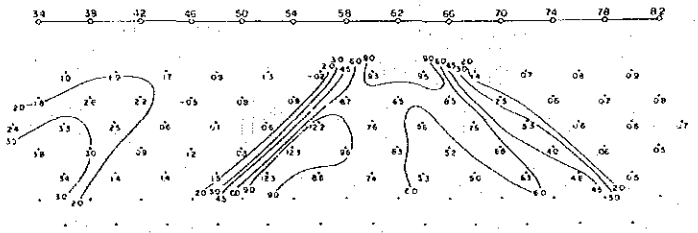

CALCULATED FREQUENCY EFFECT

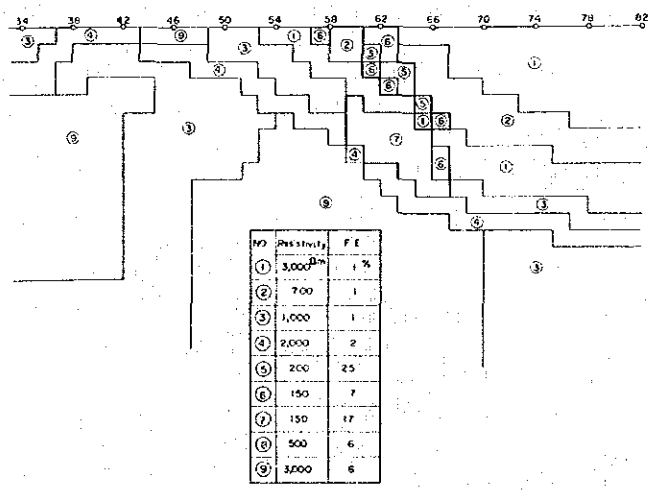

NO	Resistivity	F E
①	3,000 Ωm	1 %
②	700	1
③	1,000	1
④	2,000	2
⑤	200	25
⑥	150	7
⑦	150	17
⑧	500	6
⑨	3,000	6

SIMULATED MODEL

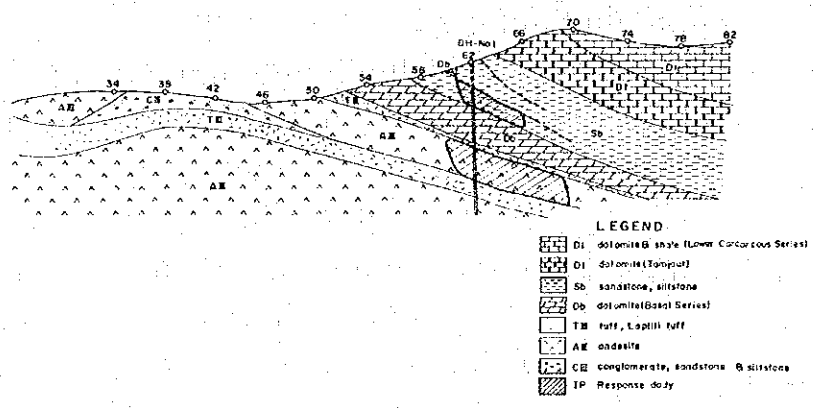

IP RESPONSE BODIES ASSUMED WITH THE GEOLOGY

Chapter 8 Correlation between Geochemical Survey and Geophysical Survey (IP method)

In the geochemical survey, the assays were made on the 3 elements of Cu, Pb, and Zn, as stated in Chapter 3, Part I. A brief summary of the results tells that Cu values are higher in the conglomerate than others in Basal Series, Pb is high in the dolomite, and Zn is lower in the dolomite and sandstone. Cu is lower in the dolomite of the Lower Calcareous Series, while Pb is higher. Pb is higher in the PII-III andesite, and Cu is higher but Pb is lower in the PIII siltstone. The rhyolite shows lower Zn.

In K Area, Pb in the dolomite of Basal Series is higher and Cu is higher in the shale. For the purpose of correlation of the geochemical assays, a distribution maps were made, based upon the assay values above 30 ppm in Cu, Pb, and Zn (cf. Figs. from II-8-1 to II-8-4). For the sake of convenience in explanation in this chapter, any assay above 30 ppm will be expressed as high value as well as FE anomaly due to the FE response body (Rt or Ra) will be expressed as FE anomaly Rt or FE anomaly Ra.

8-1 Talat-n-Sous Area

(1) FE response bodies for the FE anomalies from Rt 1 to Rt 4 are estimated in the sandstone and siltstone in Basal Series. As they are not high in Cu among Basal Series, possibility of copper deposit to exist in these rocks is very scarce, and the response bodies are considered to be pyritiferous principally.

(2) An FE response body can be estimated below the sandstone and siltstone for the FE anomaly Rt-5. The PIII conglomerate is exposed in the north side of this response body, but no sulphide has been recognized in the PIII conglomerate and the results of geochemical survey have shown that Cu in the conglomerate is not stronger than other layers of PIII formation. However, sulphides are recognized in the conglomerate of Basal Series in which Cu is specially high, as shown by the results of geochemical survey. Therefore, if the conglomerate of Basal Series exists concealedly in the ground, this FE

response body (Rt-5) may possibly be estimated to indicate sulphide dissemination or copper mineralization.

8-2 Assif Imider Area

(1) High values of Cu, Pb, and Zn were detected over the known ore deposit, which is considered the main cause for the FE anomaly Ra-1. These geochemical highs are considered to form a halo around the known ore deposit, from which correlation between the FE anomaly derived by ore deposit and geochemical highs will be made possible to discuss.

(2) On the other hand, the FE anomaly Ra-2 is considered due to the andesite exposed in the southeast of the surveyed area, but geochemical highs on Cu and Pb have not been detected around here and feeble values of Zn have been detected in stead. But nothing is clear about the entire aspect, as the location is the extremity of the surveyed area.

(3) The FE anomaly Ra-3 was estimated to be in the conglomerate, sandstone, and shale of Basal Series in the northeast of the surveyed area. High values Cu, Pb, and Zn together were recognized scatteredly in the said formation, but as to the values of Pb and Zn, considerable big difference has not been recognized between the geochemical data around the FE anomaly Ra-3 and that of the formation in the north and west parts. Around the location where the FE anomaly Ra-3 was detected, Cu showed higher values of 124 ppm - 175 ppm. Cu values in the west and north parts, where FE anomaly was not detected in the said formation, seem to be slightly lower as 41 ppm - 75 ppm. Ra-3 is estimated principally due to pyrite in the conglomerate, considering from the results of geological survey and simulation analysis, but from the geochemical results, copper mineralization is assumed to be associated for some extent.

Fig Ⅱ-8-1a GEOCHEMICAL MAP (Cu DISTRIBUTION) IN TALAT-N-SOUS

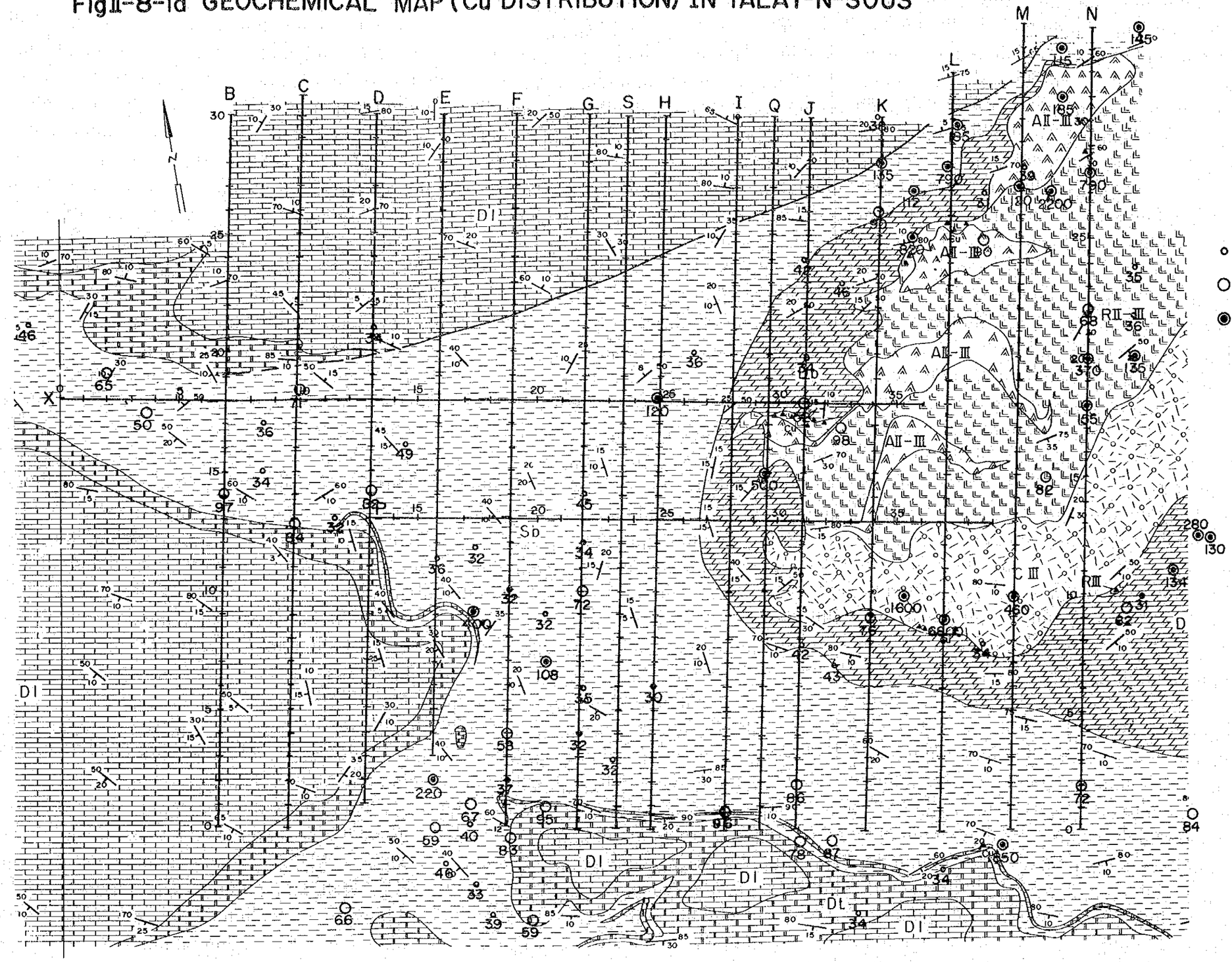

Fig II-8-1b GEOCHEMICAL MAP (Pb DISTRIBUTION) IN TALAT-N-SOUS

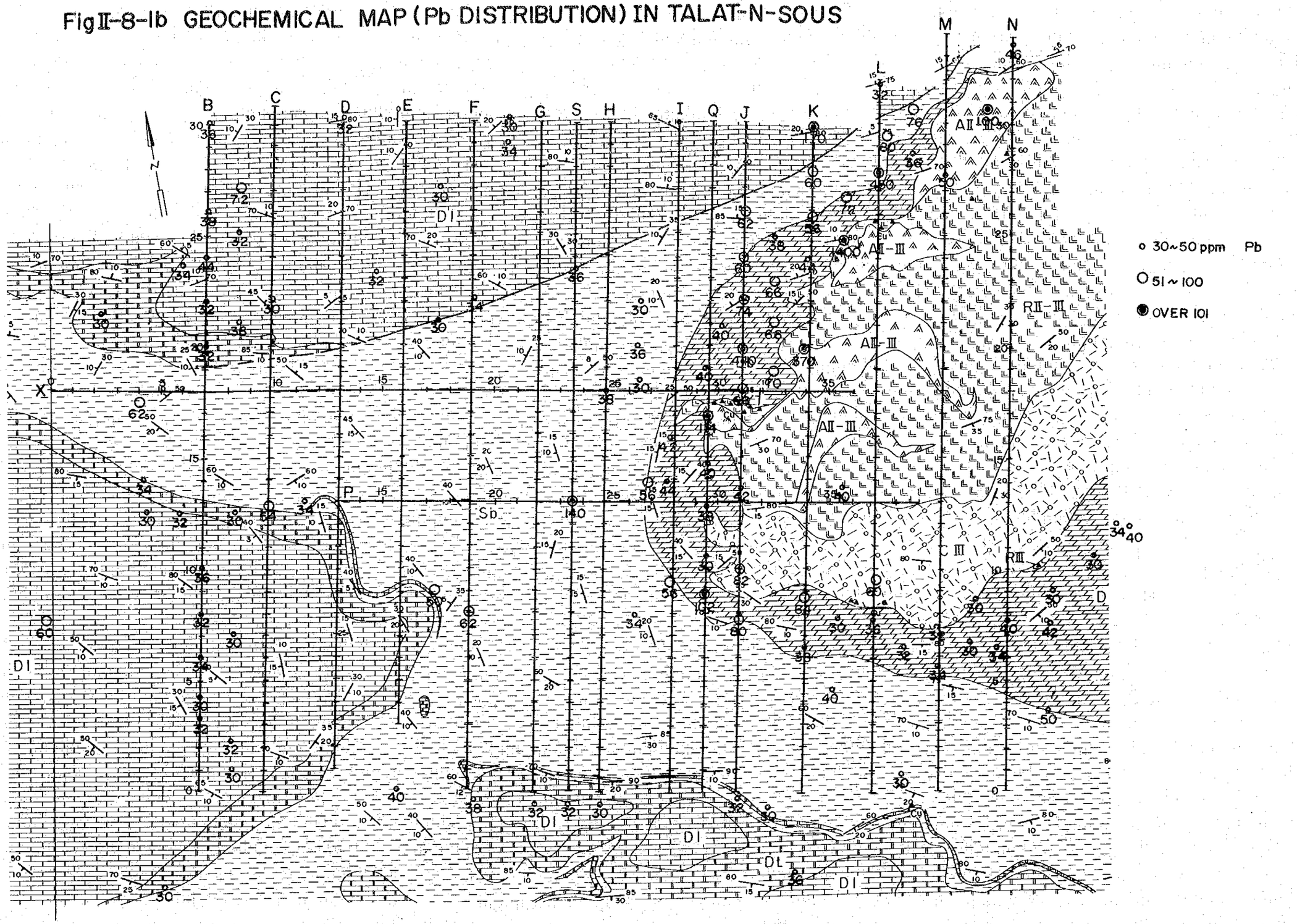

Fig II-8-1c GEOCHEMICAL MAP (Zn DISTRIBUTION) IN TALAT-N-SOUS

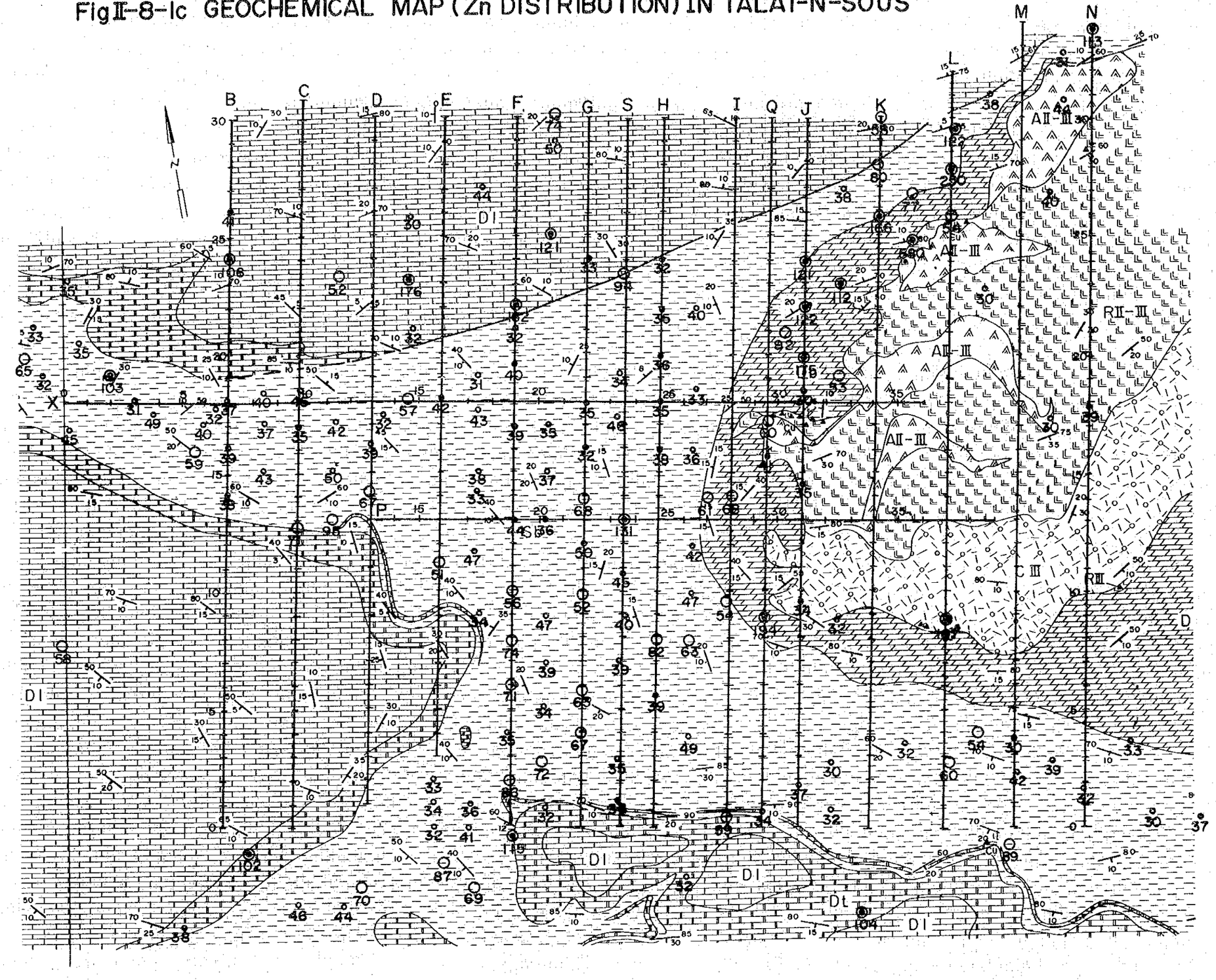

Fig II-8-2a GEOCHEMICAL MAP (Cu DISTRIBUTION) IN ASSIF IMIDER

Scale 1: 15,000

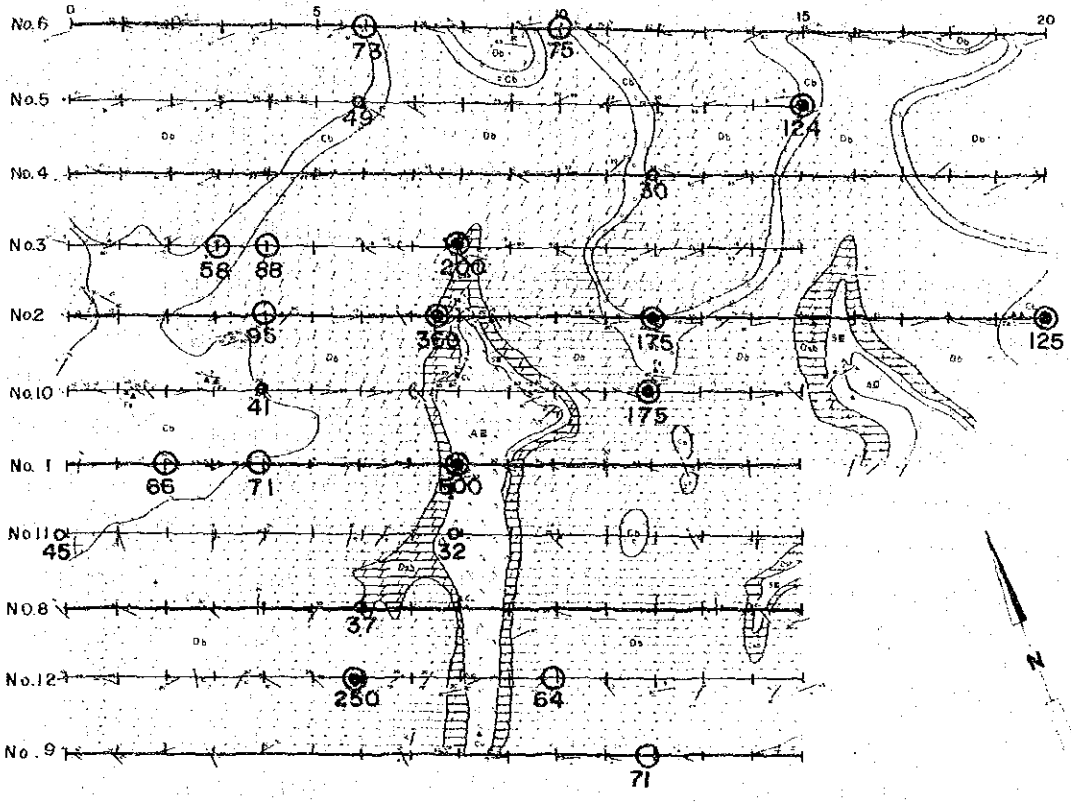

○ 30～50ppm Cu

○ 51～100

◉ OVER 101

Fig Ⅱ-8-2b GEOCHEMICAL MAP (Pb DISTRIBUTION) IN ASSIF IMIDER

Scale 1:15,000

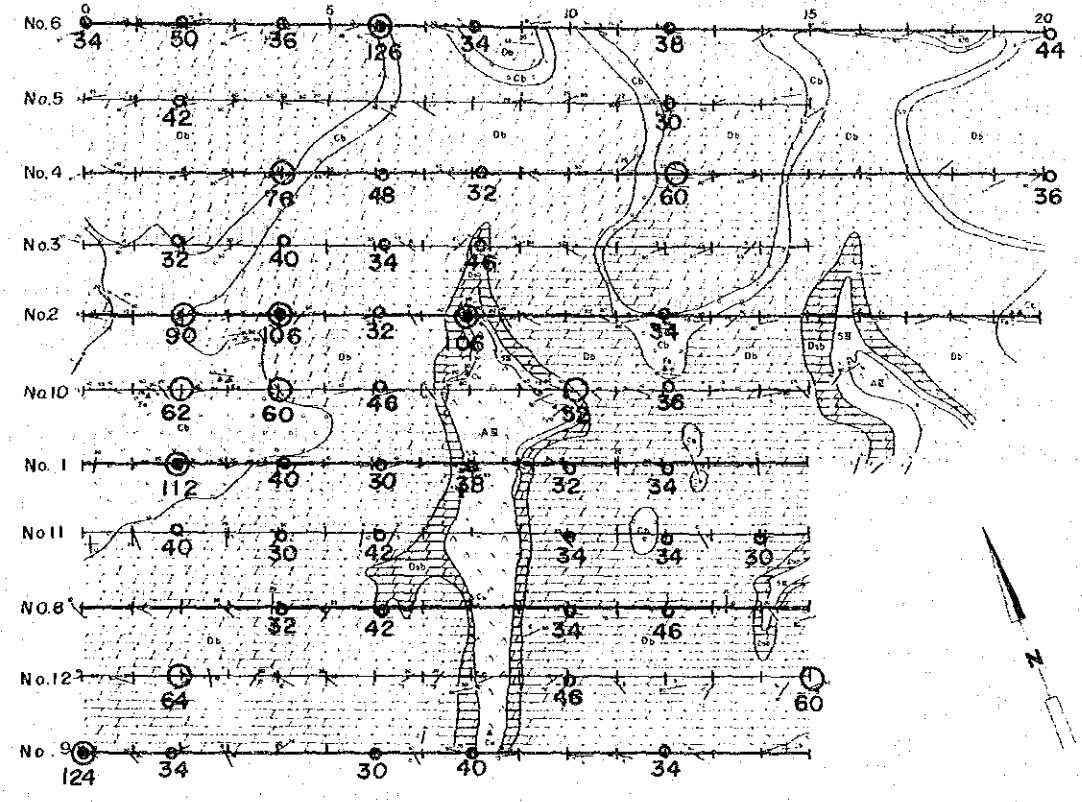

○ 30～50ppm Pb

○ 51～100

◉ OVER 101

Fig Ⅱ-8-2c GEOCHEMICAL MAP (Zn DISTRIBUTION) IN ASSIF IMIDER

Scale 1: 15,000

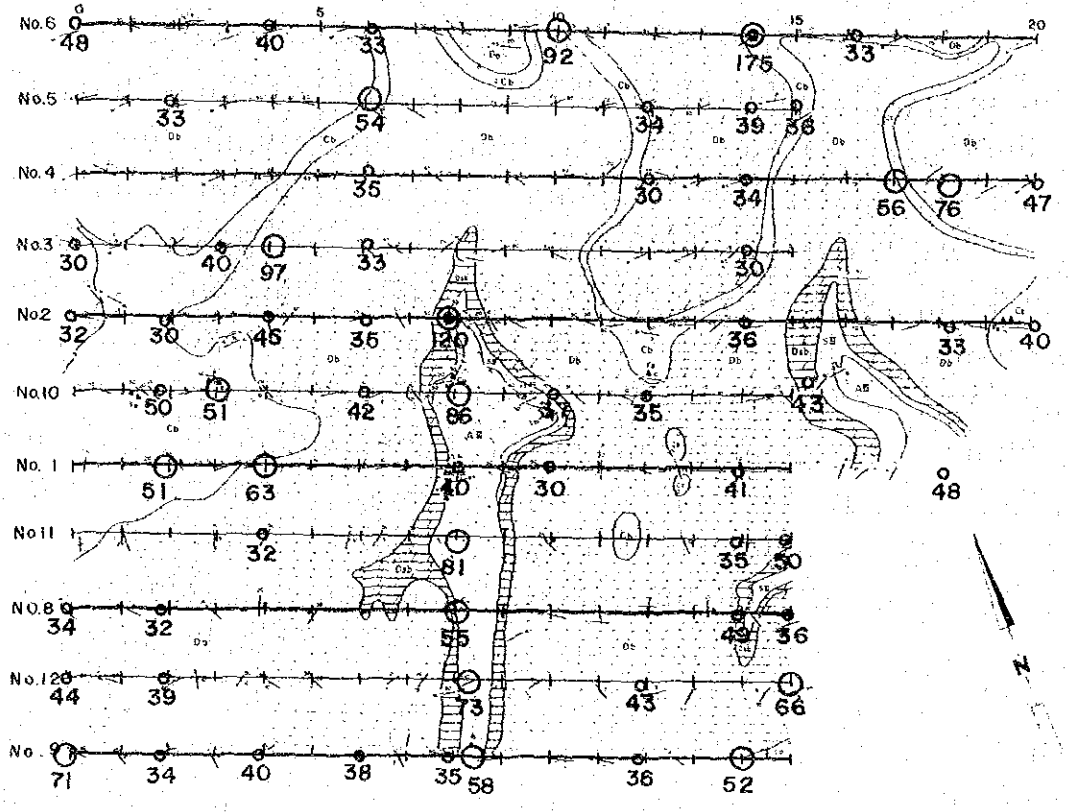

○ 30～50ppm Zn

○ 51～100

◉ OVER 101

Chapter 9 Conclusion

9-1 Talat-n-Sous Area (cf. PL II-6-10, PL II-6-11, Fig. II-6-1, Fig. II-6-2)

(1) The IP indications of similar pattern were detected near stations of 4 and 5, continuously between the survey lines K and N. Among the inferred FE response bodies (Rt-5), the small slab in the shallow ground is considered to indicate pyrite dissemination in the sandstone and siltstone, and massive or inclined prismatic body inferred deeper than the former may be interpreted in several ways, like for instance; (A) sulphides or iron oxides concentrated in the fractured zone in PIII formation, (B) iron oxides in the andesite of PII-III formation, and (C) sulphides or copper mineralization in the conglomerate of Basal Series. As the case of (C) is considered more possible, additional IP survey is necessary to be performed between the area including the Amdouz Mine and this area, and confirmation of geological structure by boring is also necessary.

(2) In the sandstone and siltstone of Basal Series, FE anomalies were detected, in which the existence of FE response bodies probably due to pyrite (Rt-1 - 3) were inferred. Among them, the FE response body (Rt-3) inferred on both sides of the doming up of high AR zone has not been duely interpreted geologically, which may necessitate the confirmation of geological structure by boring.

(3) Around the known disseminated zone principally of oxide and carbonate minerals, aggregates of very weak FE were detected in the background in response to the surface showings, for which an FE response body (Rt-4) was inferred. This was interpreted to have been caused not only by some clay minerals contained near the known zone of mineral dissemination, but also by the existence of some sulphides in the deep ground with less influence of weathering. And as this mineralized zone is estimated very small scaled, scarce possibility has been concluded in the existence of low grade, large sized copper deposit in the surroundings of Talat-n-Sous.

9-2 Assif Imider Area

(1) From the IP indications over the known ore deposit, the structure corresponding to the deposit (Ra-1) is estimated as a large scaled slab lying below a small slab in the shallow ground. The larger slab in deep shows similar physical properties to the small slab in the shallow ground. But the lack of downward persistency of the deposit has been proved by the previous boring, and according to the results of boring DH-No. 1 drilled in Alous during present survey, the response body has a strong possibility to indicate non-useful minerals principally of iron oxides distributed in the andesite. The inclined existence of this slab may indicate the ocurrence of iron oxides and others concentrated selectively in certain layer of andesite among the accumulated layers of andesite lavas, instead of mineral dissemination along a vertical fractured zone.

On the other hand, because the small slab corresponding to the ore deposit is estaimated to continue from the survey line No. 2 to the line No. 9, it is considered necessary to confirm this continuity and downward structure.

(2) Distribution of andesite, sandstone, siltstone, and conglomerate are observed on the surface of the east side of the surveyed area. As this part happens to be the southern extreme of the survey lines, the FE indications have not been detected perfectly. Therefore, additional IP survey and geochemical survey are thought necessary.

(3) The strong FE anomaly detected in the northeast of the surveyed area has suggested the existence of response body (Ra-3) as the result of simulation, through which the FE anomaly may be attributed to the pyrite disseminated zone in the formation of conglomerate, sandstone, and shale.

9-3 Conclusion

(1) The deposits of copper dissemination in the late Pre-Cambrian igneous rocks and the bedded copper-lead deposits in the Infra-Cambrian formations are the ore deposits expected in Anti Atlas region. Distinct IP indications were obtained in the Assif Imider Ore Deposit, which is a representative of the former in this surveyed area. At the same time, however, the fact of

causing a strong and wide IP anomaly by iron oxides was confirmed in Alous Area, which are locally concentrated in the igneous rock (andesite) similar to the host rock of the Assif Imider Ore Deposit.

(2) Geophysical survey by IP method has never been tried over the known ore deposit of Amdouz, emplaced in Infra-Cambrian System in this area, but its effectiveness will be expected reasonably, so with reference to other examples of IP survey, because pyrite is contained in the said formation. At the same time, however, it was also confirmed in Alous Area that strong and wide FE anomaly was caused by local concentration of pyrite contained in the conglomerate and in the alternation of sandstone, siltstone, and shale of Basal Series, though not recognized distinctly on the surface. FE anomalies of similar type to the FE anomaly of large scale were detected in Alous and the response bodies (Rt-1 - Rt-3) were inferred in Talat-n-Sous Area, and the one (Ra-3) was in Assif Imider Area.

(3) In addition, an existence of FE response body (Rt-5) was inferred in Talat-n-Sous Area through geophysical survey by IP method. Through the assumed structure by simulation and its geological interpretation, and comparison with the results of geochemical survey, this response body (Rt-5) was interpreted that possibly it might not be the one caused simply by pyrite or oxides of iron.

(4) It has been made clear by the comparison of geochemical survey adopted in the present survey and geophysical survey by IP method, that FE anomaly showed fair correlation to the geochemical results over the known ore deposits, especially closer correlation with Cu values. By comparing the results of present geophysical survey by IP method and geochemical survey over the Assif Imider Ore Deposit, an example was obtained that enabled to extract FE anomalies caused by useful minerals among the FE anomalies detected.

(5) Therefore, the prospecting procedures adopted in the present survey, such a multiple procedures of geophysical, geochemical, and geological surveys combined, to cover the areas of detailed survey, may be evaluated very effective and is believed to be adopted in future survey in the Anti Atlas region.

(6) Followings are the locations and procedures to be taken up, desired from the results of present survey;

1. Talat-n-Sous Area

(A) Geophysical survey by IP method in the area between the Amdouz Mine and present surveyed area with a total length of survey lines 15 km (1.5 km x 10 lines = 15 km), for the purpose to confirm the FE response body (Rt-5).

(B) Diamond boring for the said (Rt-5) by one drill hole for the depth of about 300 m.

(C) Diamond boring for the FE response body (Rt-3) by one drill hole for the depth of about 300 m.

(D) Diamond boring for the FE response body (Rt-2) by one drill hole for the depth of about 300 m, but optional according to the results from (C).

2. Assif Imider Area

(A) Diamond boring by one drill hole of about 200 m deep, to be located around station 8 of the survey line No. 9, for the purpose to confirm the southward continuity of FE response body (Rt-1) and structure in deep ground.

(B) Geophysical survey by IP method for FE response body (Ra-2), and detailed geochemical survey. Total length of IP survey lines for 6 km. (1.5 km x 4 lines = 6 km)

(C) Diamond boring by one drill hole of about 200 m deep, for the purpose to confirm FE response body (Ra-3). This response body is assumed to reflect pyrite in the conglomerate, but possibility of copper mineralization may not be denied in view of strong Cu values by geochemical survey. Either of which will be determined by this boring.

PART 3

PROSPECTING BORING

APPENDICES

List of Tables

List of Figures

List of Plates

Chapter 1 General Remarks of Boring

1-1 Introduction

Present bore hole, DH - No. 1, was drilled in the area of the Alous Mine where detailed geological survey and IP survey were performed during the survey of second year phase, for the purpose to investigate geological structure and the IP anomalous zone detected by the IP survey. The location of drill hole is shown by PL. III-1.

The drilling work was begun on February 16, 1977 and completed on March 7, 1977, at the drilled depth of 150 m. The hole was further drilled additionally by B.R.P.M. from March 8 and completed on March 18, 1977 at the total depth drilled of 300 m.

The drilling work was carried out by 3 drilling engineers and 18 laborers on three shift basis. The drilling machine (Longyear Type 38) and accessory materials and tools such as pumps, drilling rods, and drilling tools were borrowed from B.R.P.M. for the execution of this work.

1-2 Details of Works

1-2-1 Preparatory Works

The preparatory works required for this operations were performed under the supervision by B.R.P.M.. The works consisted of installation of drilling camp, transportation of machineries, tools, and materials, preparation of access road, clearing of the drilling site, etc. Drilling water was secured by transporting in a water truck of 5 tons capacity twice a week from Taroudannt, 35 km away from the drill site.

1-2-2 Moving Operation

As the drill site is located at an altitude of 1,100 m SL of gentle topography of hills with scarce vegetation, construction of access road of 4 m wide and 2 km long and clearing of the drill site were performed by a bulldozer and man powers. Some portions of hard exposed rocks were blasted.

1-2-3 Withdrawal Operation

At the moment of completing the drilling work on March 7, 1977, machineries and accessories were entirely returned to B.R.P.M., and all of them were re-employed in the additional drilling of the hole by B.R.P.M. started on the next day. This additional drilling was completed to have advanced to the total depth of 300 m on March 18. After pulling out casing pipes, taking off water pipes, and dismantling drilling machine on March 20, they were all sent back to the storage house in Agadir by truck.

1-2-4 Progress of Drilling Advance

The drilling work was commenced by a 3-1/2" tricone bit. NX casing pipes were inserted to the depth of 3.15 m. From this depth to the bottom, the hole was drilled by NWM diamond bits. The hole encountered a fractured zone at 32.80 m depth, which caused caving of bore hole and escape of water. Drilling was continued after preventing of escape of water with bentonite. Consequently, the escape of water was stopped at the depth of 67.55 m. Since then the hole was advanced in good condition till the depth of 95.65 m, where escape of water happened with fractures. Here, mud water of bentonite was used to prevent cavings of hole. The hole could be advanced to the bottom with scarce choking. The progress record of this hole DH - No. 1 is tabulated on Fig. III-1.

1-2-5 Core Recovery

As the overburden of the drill site was estimated about 3 or 4 m deep, the drilling was initiated by 3-1/2" tricone bit, but the hole was drilled by ordinary procedure since then.

The overburden was confirmed to the depth of 3.15 m by this drill hole. The drilling work was performed as schedule after encountering the solid rocks of Basal Series and PIII formation, which were more or less in uniform character.

Drilling bit was replaced by diamond bit in the work after the depth of 3.15 m. Mud water of bentonite was used to prevent the caving of hole during drilling.

Core recovery nearly 100 % was attained by conventional drilling method. Results of core recovery by depth is shown as follows;

Depth		Core Recovery
m	m	%
3.15	50.00	100
50.00	100.00	100
100.00	150.00	100

The cores recovered were packed in 28 core boxes made of plastics to be kept in the dried store house in the branch office of B.R.P.M. in Agadir under the supervision of B.R.P.M..

Chapter 2 Geology of Boring

2-1 Geological Environment of Drill Site

The drill site is located on the margin of Ouaonfenerha inlier elongated eastwesterly for about 10 km with the width of about 5 km in north-south. The inlier is consisted of the Pre-Cambrian PIII formation, and its outer margin is consisted of the widely distributed Infra-Cambrian formations of Basal Series, Tamjout Dolomite formation, and Lower Calcareous Series.

PIII formation consists of andesite and its pyroclastics, and is intrude by rhyolite. Basal Series consists of sandstone, siltstone, and dolomite. Lower Calcareous Series consists of dolomite.

Minerlization recognized in the surroundings is of dissemination or net-work type worked upon the rhyolite and andesite and their pyroclastics in PIII formation of the latest Pre-Cambrian. The known ore deposits of Alous, Assif-Imider, Amenayo, etc. were prospected and reported by B. R. P. M. .

The Alous Ore Deposit was so formed that copper mineralization in the rhyolite intruded into the formation of andesite and its pyroclastics was enriched advancedly along the faults and fracturedzones. A considerable amount of exploration by boring and tunneling was done, according to the report of B. R. P. M. (1968), with reported ore reserves of about 6 million tons at 0.8 % Cu. The exploration is suspended at present.

The ore deposits of Assif Imider and Amenayo are considered to have been formed by advanced secondary enrichment along the zones of weak lines, as copper mineralization is recognized near the upper part of the formation consisted of andesite and its pyroclastics.

The drill site was chosen at survey station 62 of line E, where a prismatic response body was infered more or less clearly among the continuous strong IP indications detected by the IP survey of second year phase.

2-2 Bore Hole Geology

(1) Drill Cores and Horizons

Geological succession of the bore hole examined on the cores is given as below.

Depth m	m		
3.15	85.23	Basal Series:	sandstone, alternation of sandstone and siltstone
85.23	155.50	Basal Series:	dolomite
155.50	161.50	PIII formation:	andesitic pyroclastics
161.50	232.05	" " :	andesite
232.05	265.30	" " :	andesitic pyroclastics
265.30	303.15	" " :	andesite

Alteration are read as follows;

m	m		
3.15	85.23	Basal Series:	strong sericitization
155.50	192.75	PIII formation:	strong chloritization
192.75	232.05	" " :	strong epidotization

Veinlets of quartz and calcite are recognized throughout the cores, chlorite and epidote veinlets are from the depth of 155.50 m to the bottom, and anhydrite veinlets between the depth of 208.25 m and 232.05 m, 265.00 m and 303.15 m.

Mineralization observed from the cores is remarked as follows;

m	m		
13.15	17.50	Basal Series:	dissemination of pyrite (minor)
71.15	85.23	" " :	" " (feeble)
155.50	206.60	PIII formation:	dissemination of hematite (strong)

Scattered chalcopyrite in minor amount is observed in the lower part of dolomite and feeble dissemination of malachite is observed in quartz veinlets.

Geological log of this hole is hown by PL. III-2.

Fig. Ⅲ-1 Drilling Progress, DH-No. 1

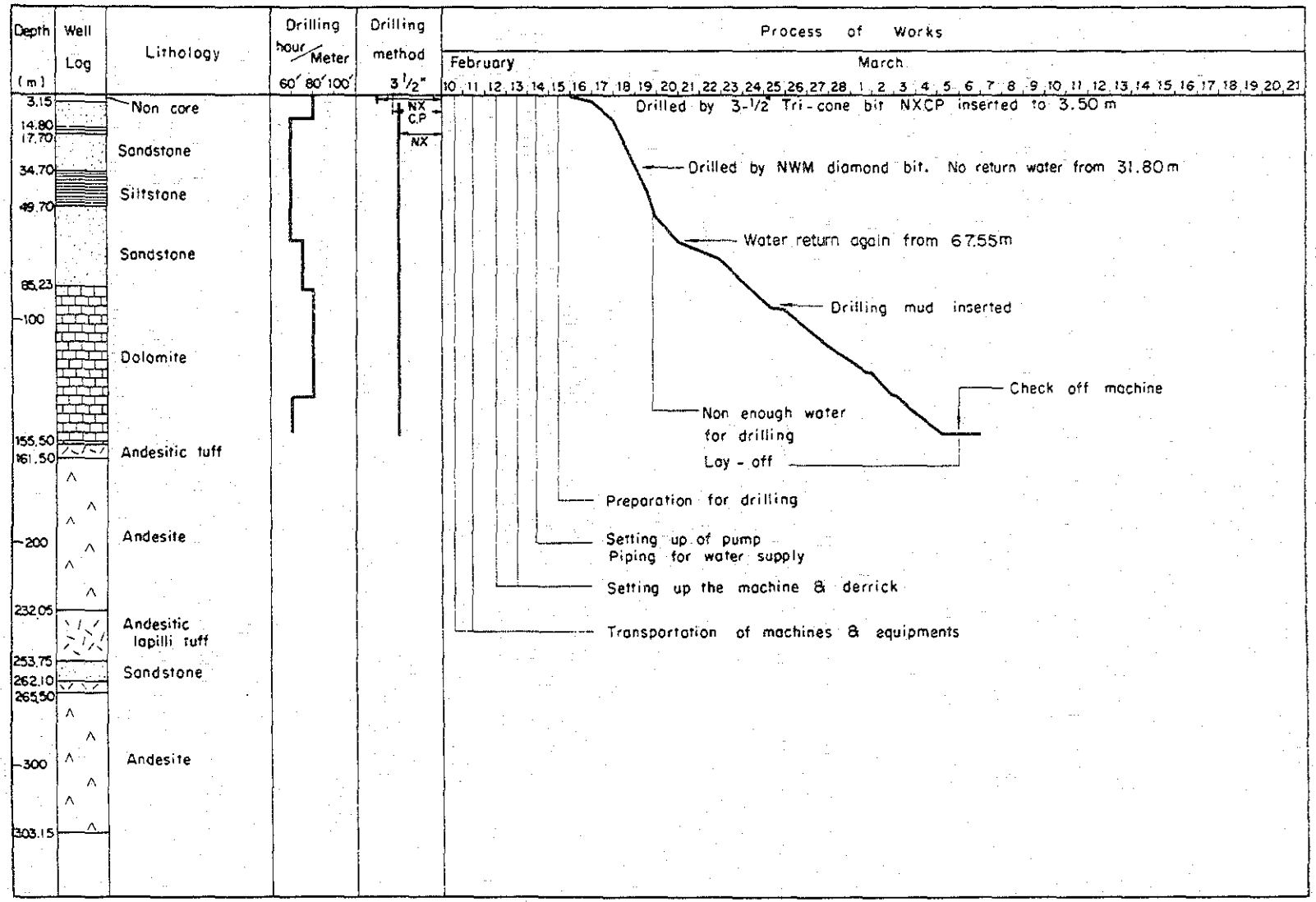

Chapter 3 Results of Boring

3-1 Relation with the Survey of Second Year Phase

The Infra-Cambrian Basal Series has been confirmed by this drill hole between the depth of 0 m and 155.50 m and Precambrian PIII formation from the depth of 155.50 m to 303.15 m (the bottom), which nearly coincide to the geological profile made through the detailed survey of second year phase. (cf. PL. III-1).

In view of existence of copper mineralization in the uppermost part of andesite of PIII formation as the results of detailed geological survey in this area, copper mineralization was expected in this drill hole, but only the dissemination of hematite (specularite) was found as its result.

3-2 Correlation with the Data of Geophysical Survey

The anomalous zones detected by the IP survey in the second year phase are as follows;

(1) FE anomalous zone possibly derived by copper minerlization in the rhyolite intrusive in the Alous Mine,

(2) FE anomalous zone of unknown origin near the contact between the formation of andesite and its pyroclastics of the PIII and Basal Series,

(3) FE anomalous zones inferred in the sandstone in the lower part of Basal Series and andesite formation in PIII formation.

The distribution patterns of these anomalies show distinct roof shapes, and the response bodies inferred from the FE distribution are horizontal slab, inclined slab and massive in their shapes. The Alous Mine in which considerable exploration works were done by B.R.P.M. is indicated by one of these anomalous zones. The present boring was performed for the purpose to investigate the origin of FE anomaly detected in Basal Series.

The drill site, survey station 62 on survey line E, is the location where the most distinct FE anomalous zones were detected.

Considering them in correspondence to the drilling results, the response body near the surface corresponds to the sandstone of Basal Series where weak dissemination of pyrite and hematite is accompanied. The response body reaching to the deeper ground with prismatic shape corresponds to weak dissemination of hematite in the andesite. Copper mineralization has not been recognized in both of the response bodies.

The results of laboratory measurement of FE and AR values are shown by Fig. III-2. To mention them by rock types, those of sandstone, siltstone, and dolomite of Basal Series coincide to the values of in-situ measurement, but are different in andesite. FE values are generally high, and the sandstone with pyrite impregnation shows FE values up to 25 % in shallow ground of 10 m deep, while FE value of the sandstone in the depth from 60 m to 80 m is a little less than 5 %. The hematite (specularite) bearing andesite existing deeper than 160 m has fairly dispersed FE values from about 20 % to less than 2 %, which is considered to have caused by heterogeneous distribution of iron minerals contained in the andesite.

Fig. Ⅲ-2 Distribution of F.E. & A.R. in Depth

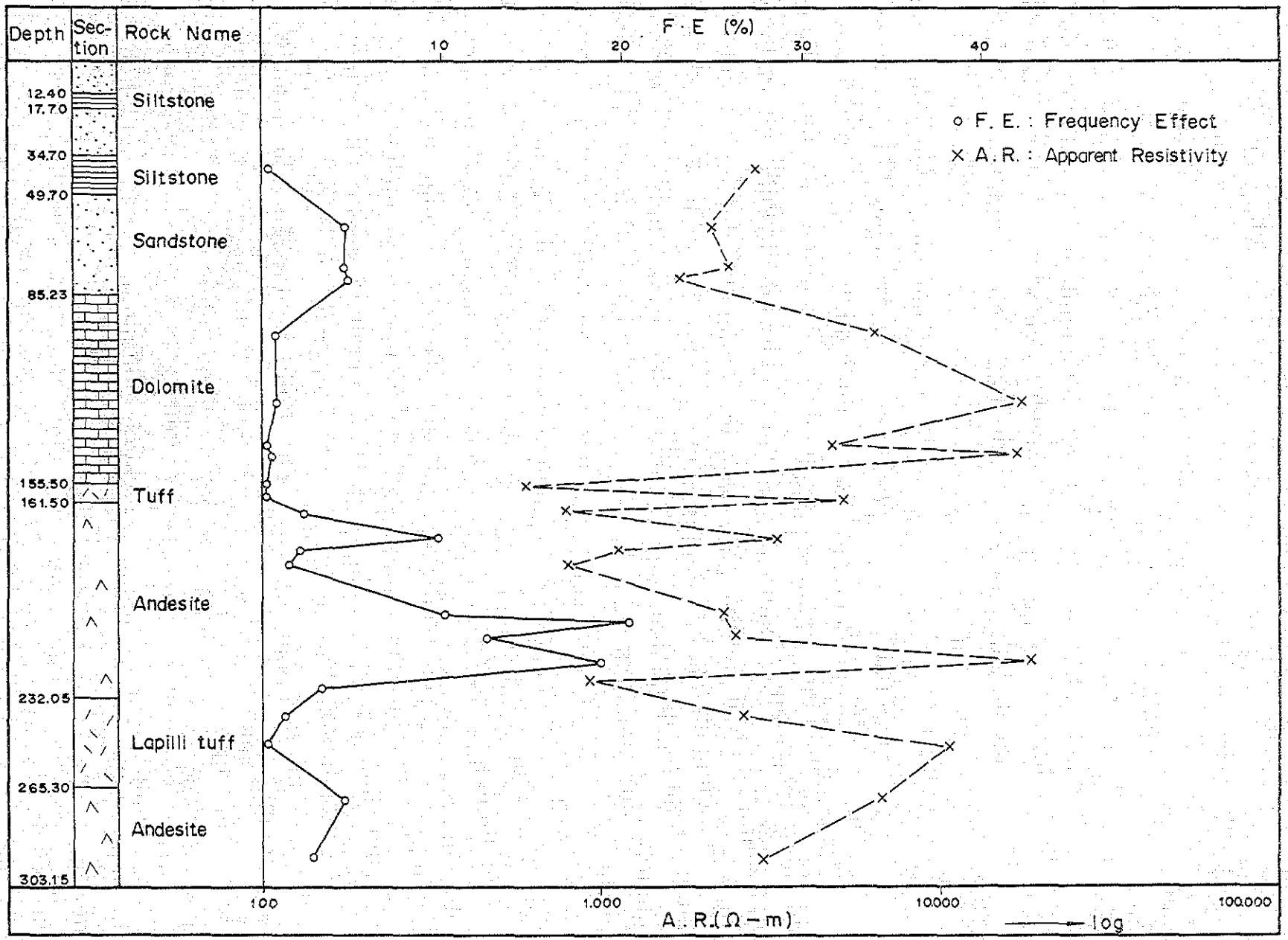

Chapter 4 Conclusion

(1) This boring was carried out in the area of the Alous Mine for the purpose of investigating the geological structure and FE anomaly obtained through detailed geological survey and IP survey performed in the second year phase.

(2) The drill site is located in the marginal zone of Ouaonfenerha inlier. The inlier consists of the Pre-Cambrian PIII formation and its marginal zone consists of the widely distributed Infra-Cambrian Basal Series, Tamjout Dolomite formation, and Lower Calcareous Series.

(3) Types of mineralization found around the present survey areas are dissemination and network types in the rhyolitic and andesitic rocks in PIII formation corresponding to the latest Pre-Cambrian. The ore deposits of Alous and Assif Imider are noted as the known ore deposits.

(4) The drill site is survey station 62 on the survey line E, where continuous and strong anomalous zones were detected by IP survey performed in the second year phase.

(5) The drill hole geology almost coincides to the geological profile prepared for the report of the second year phase.

(6) Copper mineralization was expected in the uppermost part of the PIII andesite as the result of geological survey, but dissemination of hematite (specularite) was only found by this boring.

(7) According to the IP survey, the IP indication showed a distinct roof shaped pattern, from which the response bobies of horizontal slab and massive body were inferred with reference to the distribution of FE anomalies.

(8) The results of boring revealed that one of the response body was caused by weak dissemination of pyrite and hematite contained in the sandstone of Basal Series, and the other massive response body was estimated to have been caused by weak dissemination of hematite (specularite) in the andesite.

(9) According to the results of present boring, copper mineralization was scarcely recognized in the FE anomalous zone detected in the lower part of Basal Series.

APPENDICES

(GEOLOGICAL SURVEY)

Table I-1 List of Rock Samples (1)

Location (Area)	Sample No.	Field Observation	Thin Section	Polished Section	Mineral Analysis				Chemical Analysis	X-ray Analysis	Dating	Remarks
					Ag	Cu	Pb	Zn				
H	B-11	Conglomerate										
H	B-15	Andestic Sandstone										
H	B-16	Andestic Sandstone	○									Photo No. 1
H	B-50	Dolomite										
H	B-51	Sandstone										
H	B-52	Shale				○	○	○				
H	B-54	Rhyolite										
H	B-55	Rhyolite										
H	B-56	Rhyolite										
H	E-13	Shale (py)	○									
H	E-15	Shale (mala)										
H	E-16	Shale (mala)	○									
H	E-17	Andesite										
H	E-18	Dolomite (mala)										
H	E-19	Shale (mala)			○	○						
H	E-21	Siltstone										
H	E-22	Andesite (trachytic)	○						○			Photo No. 2
H	E-122	Rhyolitic tuff								○		

Location (Area)	Sample No.	Field Observation	Thin Section	Polished Section	Mineral Analysis				Chemical Analysis	X-ray Analysis	Dating	Remarks
					Ag	Cu	Pb	Zn				
H	E-126	Rhyolitic tuff										
H	E-127	Rhyolitic tuff	O									Photo No. 3
H	E-128	Rhyolite (mala)										
H	E-129	Rhyolite	O						O		O	
H	E-130	Rhyolite (mala)			O	O						
H	E-131	Rhyolite (mala)			O	O						
H	E-137	Dolomite (mala-cc)		O								
H	F-105	Rhyolite (mala-cc)		O								
H	F-107	Andesite dyke	O									
H	F-108	Andesitic conglomerate								O		
H	F-113	Rhyolitic tuff	O									
H	F-114	Rhyolitic lapilli tuff	O									
H	F-115	Rhyolitic tuff (mala-cc)										
H	F-146	Siltstone (mala)								O		
H	F-148	Rhyolitic lapilli tuff										
H	F-150	Andesite (mala)	O									Photo No. 4

Location (Area)	Sample No.	Field Observation	Thin Section	Polished Section	Mineral Analysis				Chemical Analysis	X-ray Analysis	Dating	Remarks
					Ag	Cu	Pb	Zn				
H	F-152	Rhyolitic tuff										
H	F-153	Rhyolitic lapilli tuff										
H	F-154	Sandstone										
H	F-161	Dolomite (mala)										
H	F-162	Sandstone										
H	F-166	Dolomite										
H	F-169	Dolomite										
H	F-170	Conglomerate										
H	G-29	Andesite										
H	G-30	Rhyolite	○									
H	G-31	Andesite	○									
H	G-32	Andesite	○						○			
H	G-34	Conglomerate (mala)										
H	G-35	Dolomite (mala)								○		
H	G-36	Dolomite	○									
H	G-37	Rhyolite	○						○		○	
H	G-49	Rhyolitic sandy tuff	○									Photo No. 5
H	G-51	Sandstone								○		

Location (Area)	Sample No.	Field Observation	Thin Section	Polished Section	Mineral Analysis				Chemical Analysis	X-ray Analysis	Dating	Remarks
					Ag	Cu	Pb	Zn				
H	G-52	Sandstone								○		
H	G-54	Rhyolitic tuff										
H	G-55	Porphyritic andesite	○									
H	G-56	Brecciated andesite	○									
H	G-57	Basic andesite	○									
J	B-17	Rhyolite										
J	B-18	Rhyolite	○									
J	B-21	Andestic tuff breccia	○									
J	B-26	Andestic lapilli tuff										
J	E-23	Andesite	○						○			
J	E-25	Rhyolite	○									
J	E-26	Rhyolite										
J	E-29	Rhyolitic tuff Lapilli tuff	○							○		PhotoNo.10
J	E-30	Rhyolite								○		
J	E-31	Rhyolitic tuff (mala)										
J	E-34	Rhyolite (mala-cc)		○								

Location (Area)	Sample No.	Field Observation	Thin Section	Polished Section	Mineral Analysis				Chemical Analysis	X-ray Analysis	Dating	Remarks
					Ag	Cu	Pb	Zn				
J	E-42	Rhyolitic lapilli tuff										
J	E-47	Andesitic tuff lapilli tuff	○									
J	E-50	Andesitic fine tuff	○									
J	E-51	Rhyolitic tuff								○		
J	E-53	Rhyolitic tuff										
J	E-60	Rhyolitie								○		
J	E-65	Andesite	○									
J	E-67	Rhyolitic tuff (mala)			○	○						
J	E-68	Rhyolite (mala)			○	○						
J	E-69	Rhyolite (mala)	○									
J	E-70	Rhyolitic lapilli tuff ~ tuff										
J	E-71	Rhyolite			○	○						
J	E-72	Rhyolite (ccp-cc)			○	○						
J	E-74	Rhyolite								○		
J	E-75	Rhyolitic tuff lapilli tuff (mala)			○	○						
J	E-76	Rhyolitic lapilli tuff	○							○		

Location (Area)	Sample No.	Field Observation	Thin Section	Polished Section	Mineral Analysis				Chemical Analysis	X-ray Analysis	Dating	Remarks
					Ag	Cu	Pb	Zn				
J	E-77	Rhyolitic tuff lapilli tuff (mala)										
J	E-78	Rhyolitic tuff lapilli tuff								O		
J	E-79	Rhyolite (mala)			O	O						
J	E-80	Rhyolitic tuff (mala)			O	O						
J	E-84	Rhyolite (mala)			O	O						
J	E-85	Rhyolite (mala)			O	O						
J	E-87	Dolomite&rhyolitic lapilli tuff (mala-cc)			O	O						
J	E-88	Rhyolitic lapilli tuff (az-mala)			O	O						
J	E-91	Rhyolitic tuff breccia (mala)			O	O						
J	E-94	Dolomite (mala)			O	O						
J	E-96	Rhyolite (mala-az)			O	O						
J	E-97	Rhyolite (mala)			O	O						
J	E-99	Rhyolite								O		
J	E-100	Rhyolite (mala)			O	O						
J	E-101	Rhyolite (mala)			O	O						

Location (Area)	Sample No.	Field Observation	Thin Section	Polished Section	Mineral Analysis				Chemical Analysis	X-ray Analysis	Dating	Remarks
					Ag	Cu	Pb	Zn				
J	E-103	Rhyolite (mala-cc)			○	○						
J	E-105	Rhyolitic tuff										
J	E-106	Rhyolite&rhyolitic tuff (mala-cryso-colla)		○								
J	E-107	Rhvolite&rhyolitic tuff (mala-az)			○	○						
J	E-109	Rhyolite (mala-crysocolla)			○	○						
J	E-111	Rhyolite (mala-az)			○	○						
J	E-112	Rhyolite	○									
J	E-113	Rhyolite (mala-az)			○	○						
J	E-114	Rhyolite (mala-cc)			○	○						
J	E-116	Rhyolite (mala-az)			○	○						
J	E-117	Rhyolite (mala)			○	○						
J	F-118	Rhyolitic Sandston	○									
J	F-119	Brecciated ande-site	○						○			
J	F-120	Rhyolitic tuff (mala)										
J	F-123	Rhyolite	○						○			
J	F-134	Rhyolitic lapilli tuff	○									

Location (Area)	Sample No.	Field Observation	Thin Section	Polished Section	Mineral Analysis				Chemical Analysis	X-ray Analysis	Dating	Remarks
					Ag	Cu	Pb	Zn				
J	F-137	Rhyolitic lapilli tuff	○									
J	F-139	Andesite										
J	F-141	Andsitic fine tuff	○									
J	F-142	Rhyolitic tuff										
J	G-38	Rhyolite	○									Photo No.11
J	G-39	Andesite	○									Photo No.12
J	G-40	Andsitic tuff										
J	G-41	Andesite	○									Photo No.13
J	G-42	Tuff										
J	G-43	Rhyolite (mala)								○		
J	G-44	Micaceous sand-stone	○									
J	G-45	Rhyolite rhyolitic tuff (mala)										
J	G-60	Rhyolite~rhyolitic tuff	○						○		○	
K	C-85	Dolomite										
K	C-87	Andesite	○									
K	C-88	Tuffaceous shale	○									
K	C-89	Dolomite										

Location (Area)	Sample No.	Field Observation	Thin Section	Polished Section	Mineral Analysis				Chemical Analysis	X-ray Analysis	Dating	Remarks
					Ag	Cu	Pb	Zn				
K	C-90	Dolomite										
K	Y-37	Sandstone										
K	Y-38	Andesite	○						○	○		
K	Y-39	Sandstone										
K	Y-40	Andesitic lapilli tuff										
K	Y-41	Sandstone										
K	Y-43	Dolomite	○		○	○				○		
K	Y-45	Andesitic tuff (mala-az)								○		
I	B-1	Rhyolite										
I	B-6	Rhyolite										
I	B-7	Dolomite (mala)										
I	B-8	Sandstone (mala)										
I	B-9	Andesite								○		
I	C-2	Dolomite										
I	C-4	Dolomite										
I	C-6	Dolomite										
I	C-8	Shale	○									
I	C-13	Conglomerate										

Location (Area)	Sample No.	Field Observation	Thin Section	Polished Section	Mineral Analysis				Chemical Analysis	X-ray Analysis	Dating	Remarks
					Ag	Cu	Pb	Zn				
I	C-14	Quartzite	O									Photo No. 6
I	C-15	Quartzite										
I	C-17	Rhyolitic tuff										
I	C-19	Rhyolitic tuff	O									
I	C-20	Conglomerate										
I	C-30	Pelitic schist	O									
I	D-3	Dolomite										
I	D-5	Sandstone										
I	D-6	Conglomerate										
I	D-7	Sandstone										
I	D-20	Rhyolite	O						O		O	Photo No. 7
I	E-1	Dolomite (mala)	O									
I	E-2	Rhyolite (dyke)	O									
I	E-5	Sandstone (mala)										
I	E-6	Sandstone (mala)	O			O	O	O				Photo No. 8
I	E-7	Conglomerate (mala)										
I	E-8	Conglomerate (mala)										
I	E-9	Slate	O									

Location (Area)	Sample No.	Field Observation	Thin Section	Polished Section	Mineral Analysis				Chemical Analysis	X-ray Analysis	Dating	Remarks
					Ag	Cu	Pb	Zn				
I	E-12	Conglomerate	○									
I	F-14	Siltston										
I	F-16	Sandstone	○									
I	F-21	Conglomerate	○									
I	F-33	Rhyolite	○									Photo No. 9
I	F-34	Andesite										
I	G-4	Sandy tuff										
I	G-12	Andesite										
I	G-17	Weakly welded tuff										
I	G-19	Sandstone	○									
I	G-24	Weakly welded pumice tuff										
I	Y-1	Sandstone	○									
I	Y-4	Shale										
I	Y-8	Rhyolite										
I	Y-9	Rhyolite										
I	Y-10	Rhyolite										
I	Y-11	Rhyolitic lapilli tuff	○									
I	Y-46	Rhyolite										

Location (Area)	Sample No.	Field Observation	Thin Section	Polished Section	Mineral Analysis				Chemical Analysis	X-ray Analysis	Dating	Remarks
					Ag	Cu	Pb	Zn				
L	C-55	Sandstone				○	○	○				
L	C-56	Rhyolitic tuff	○									
L	C-59	Rhyolite										
L	C-63	Conglomerate	○									
L	C-64	Conglomerate										
L	C-66	Sandstone										
L	C-70	Conglomerate										
L	C-72	Rhylitic tuff										
L	C-74	Sandstone		○		○	○	○				
L	C-76	Rhyolite	○									
L	C-77	Rhyolite										
L	C-79	Conglomerate	○									
L	C-80	Conglomerate										
L	C-81	Rhyolite										
L	C-82	Sandstone				○	○	○				
L	C-83	Andesite	○									
L	D-11	Andesite										
L	D-12	Rhyolite		○		○	○	○				
L	D-13	Trachytic tuff	○									
L	D-19	Rhyolite	○						○		○	PhotoNo.14

Location (Area)	Sample No.	Field Observation	Thin Section	Polished Section	Mineral Analysis				Chemical Analysis	X-ray Analysis	Dating	Remarks
					Ag	Cu	Pb	Zn				
L	Y-25	Conglomerate			○	○						
L	Y-26	Rhyolitic lapilli. tuff	○									
L	Y-27	Rhyolite										
L	Y-30	Conglomerate										
L	Y-32	Rhyolite										
L	Y-34	Sandstone	○									
L	Y-36	Dolomite	○									
M	C-32	Andesite										
M	C-33	Andesite	○						○	○		
M	C-34	Andesitic tuff breccia	○									
M	C-35	Sandstone	○									
M	C-36	Rhyolitic lapilli tuff										
M	C-37	Rhyolitic tuff										
M	C-38	Andesite										
M	C-39	Andesite	○									Photo No.15
M	C-41	Andesite	○									Photo No.16
M	C-42	Rhyolitic lapilli tuff										

Location (Area)	Sample No.	Field Observation	Thin Section	Polished Section	Mineral Analysis				Chemical Analysis	X-ray Analysis	Dating	Remarks
					Ag	Cu	Pb	Zn				
M	C-43	Andesite	○						○			
M	C-44	Andesite		○								
M	C-45	Rhyolitic tuff	○									
M	C-47	Sandstone										
M	C-48	Andesite										
M	C-49	Conglomerate										
M	C-50	Rhyolitic tuff	○									
M	C-51	Sandstone										
M	C-52	Rhyolitic tuff										
M	Y-16	Rhyolitic tuff										
M	Y-17	Andesite	○									
M	Y-18	Andesite										
M	Y-19	Andesite										
M	Y-20	Rhyolite										
M	Y-21	Andesite										

mala : malachite

cc : chalcocite

az : azurite

Table I-2-1 Microscopic Observation of Thin Sections

(1)

Location (Area)	Sample No.	Formation	Rock Name	Microscopic Observations	Remarks
H	B-16	PIII	Volcanic feldspathic sandstone	Well sorted, subangular grains of stippled feldspar, quartz, and carbonate and trachytic to andesitic pumiceous fragments are packed in tuffaceous materials pigmented with reddish opaque minerals.	See microphoto. No.1
H	E-13	Basal Series	Sandy shale with pyrite	Detrital angular quartz grains, flakes of mica, and chlorite are set in a clay matrix. Calcite is often observed. Euhedral opaque mineral (pyrite?) are present. There is a weak lamination or orientation.	
H	E-16	Basal Series	Dolomitized rhyolitic tuff	Dominant angular quartz and subordinate feldspar grains are dispersed in a fine-grained dolomite grains. Red-brown mineral (hematite) and euhedral opaque minerals are often observed.	
H	E-22	PIII	Andesite	Large phenocrysts of plagioclase and mafic minerals are set in a groundmass consisting of intergranular and intersertal plagioclase laths and pigmented glass. Mafic minerals are completely altered to calcite, serpentine, chlorite, and opaque minerals. Plagioclase is albitized and sericitized.	See microphoto. No.2
H	E-127	PIII	Rhyolitic tuff	Phenocrysts of feldspars and quartz are set in a cryptofelsic base with well preserved glass shard outlines. Feldspar is partly sericitized.	See microphoto. No.3
H	E-129	PIII	Rhyolite	Large phenocrysts more than 1 mm in size of quartz, partly corroded, and feldspar are set in a devitrified, cryptofelsic groundmass with small quantities of sericite, carbonate, and opaque minerals.	
H	F-107	PIII	Altered andesite	The rock is completely altered to an aggregate of carbonates, chlorite, Ti-minerals, opaques, epidote, and minor quartz and feldspars. Mafic minerals retain euhedral outline, although completely altered.	
H	F-113	PIII	Dacitic lithic tuff	Fragments of andesite and broken crystals of feldspar, minor quartz, and altered mafic minerals are in a devitrified, cryptofelsic matrix showing relict glass shard outlines. The andesite fragments consist of dominant plagioclase laths with intersertal and intergranular fabrics.	
H	F-114	PII-III	Rhyolitic tuff breccia	Broken, corroded quartz crystals, stippled feldspar grains, pumice, altered mica flakes, and rhyolitic to andesitic rock fragments are in a cryptocrystalline matrix of quartz, sericite, clay minerals, and opaques.	
H	F-150	PIII	Altered dolerite	The rock is composed mainly of ophitic plagioclase laths and intergranular pyroxene pseudomorphs. Pyroxene? is completely altered to an aggregate of carbonate and chlorite or serpentine. Ti-Fe minerals are abundantly segregated.	See microphoto. No.4
H	G-30	PIII	Tuffaceous shale	The rock show sparse fragments mainly of quartz, plagioclase, K-feldspar, biotite, andesite, meta quartzite and rhyolite in a fine matrix of siliceous materials. Many plagioclase crystals are altered to aggregates of sericite, and vermiculite replaces biotite.	

Location (Area)	Sample No.	Formation	Rock Name	Microscopic Observations	Remarks
H	G-31	PIII	Altered dolerite	The rock consists chiefly of altered mafic minerals and plagioclase ophitically intergrown. Some of the mafic minerals are completely altered to carbonates; others are altered to chlorite and serpentine, which may be pyroxenes. Hematite and magnetite or ilmenite are segregated.	
H	G-32	PIII	Altered dolerite	The rock consists mainly of plagioclase, chlorite, carbonate and opaque minerals. Plagioclase measures 0.5 to 1.0 millimeters in size and exhibits euhedral lath-shaped crystals. Chlorite forms a psudomorph of ophitic mafic minerals, and opaque minerals also fills interstices of plagioclase crystals. The texture is automorphic ophitic. Sericite replaces plagioclase as a secondary mineral.	
H	G-36	Basal Series	Quartzose dolomitic limestone	Subangular quartz grains about 0.1 mm in size are dispersed in uquigranular dolomite mosaic. Patches of finer-grained carbonate and quartz are present.	
H	G-37	PII-III	Rhyolitic crystal tuff	Broken crystals of feldspars and quartz are set in a devitrified, carbonated, and stippled matrix of glass dusts.	
H	G-49	PIII	Graywacke sandstone	An unsorted aggregate of angular grains of crystals is set in an argillaceous material. Grains measure 0.1 to 0.3 millimeters in size and are of quartz, plagioclase, K-feldspar, mica, sphene, tourmaline and opaque minerals. Rock fragments also occur in a small amount. Carbonate is dispersed in the specimen.	See microphoto. No.5
H	G-55	PIII	Rhyolitic lithic tuff	Small amounts of quartz and feldspar grains are in a cryptofelsic matrix with glass shard relics. A few andesite fragments and euhedral opaque minerals are present.	
H	G-56	PIII	Amygdule-rich latite	Phenocrysts are made up mainly of plagioclase and opaque minerals and ranges from 0.2 to 1.0 millimeters in size. Primary minerals in the groundmass are plagioclase, K-feldspar, quartz and opaque minerals. Chlorite occurs in interstices of feldspar crystals in the groundmass and is a replacement of mafic igneous minerals. Amygdules consist mainly of quartz.	
H	G-57	PIII	Highly altered rock rich in quartz and epidote (originally diorite?)	Hornblende and opaque minerals occurs as relict primary minerals but in small amounts. Hornblende exhibits interstitial poikilitic crystals, indicating that the original rock in igneous in origin. Secondary minerals are epidote, quartz and rarely sericite.	
I	C-8	Basal Series	Shale	Fragments of quartz, plagioclase, mica and opaque minerals are sparsely scattered in a fine argillaceous material. Carbonate is formed in an authegenic material.	
I	C-14	PII	Quartzite	The rock consists almost entirely of subrounded to subangular, poorly sorted, detrital quartz grains. Outergrowths of authigenic quartz are less common. Small amounts of opaque minerals, apatite, zircon, sericite, and feldspar are present.	See microphoto. No.6
I	C-19	PIII	Rhyolitic crystal tuff	Broken crystals of quartz, orthoclase, and oligoclase are set in a devitrified, cryptofelsic base.	

Location (Area)	Sample No.	Formation	Rock Name	Microscopic Observations	Remarks
I	C-30	PII	Silicified rhyolitic tuff	Fragments are mainly of plagioclase and sparsely of K-feldspar and meta quartzite. The matrix is composed of devitrified fine grained material. Secondary minerals include quartz, albit, sphene and epidote.	
I	D-20	PII-III	Porphyry	Phenocrysts measures about 0.5 millimeters in size and are mainly of plagioclase. The groundmass minerals are quartz, plagioclase and opaque minerals, ranging from 0.1 to 0.3 millimeters in size. Quartz, albite, sphene, carbonate and epidote also occur as secondary minerals.	See microphoto. No.7
I	E-1	Lower Calcareous Series (Tarajout)	Quartz-dolomite rock (mineralized)	Veinlets and clots consisting of quartz are in an equigranular dolomite mosaic. Bluish green Cu-minerals (malachite) are associated with radiated quartz crystals.	
I	E-2	PII-III	Rhyolitic crystal tuff	Broken crystals of quartz and feldspar, together with andesitic fragments are in a carbonated matrix consisting of glass shards and dusts with minor opaques.	
I	E-6	PII-III	Volcanic sandstone	Poorly sorted andesitic to trachytic fragments, subangular quartz grains, and quartzite fragments are packed in a matrix consisting of chlorite, sericite, quartz, and carbonate.	See microphoto. No.8
I	E-9	PII-III	Sandy shale	The rock is composed of fine-grained angular detrital quartz, small amounts of feldspar grains, and sericite flakes set in clayey matrix. Opaque minerals are fairly common. The sericite flakes show a weak orientation.	
I	E-12	PIII	Rhyolitic tuff	The rock shows fragments of plagioclase, K-feldspar, quartz, granite, low grade shist, meta quartzite and andesite in a fine base of devitrified materials. The base partly shows a vitriclastic texture. Phenocrysts of quartz, plagioclase and K-feldspar are observed. Secondary minerals are sericite, calcite and chlorite.	
I	F-16	PIII	Volcanic sandstone	Poorly sorted subangular grains of andesite, rhyolite, trachyte, pumice, quartz, and feldspar are cemented by fine-grained quartz and clay minerals. Feldspar grains are lightly stippled with cleavage.	
I	F-21	PII-III	Volcanic conglomerate	Fragments of rhyolitic and andesitic rocks and chert are contained in a chloritized, sericitized, and carbonated matrix. Opaque minerals are fairly abundant. Epidote is observed.	
I	F-33	PIII	Rhyolitic vitric tuff	Broken angular crystals of quartz and feldspar less than 0.5 mm in size are set in a devitrified, cryptofelsic base. Feldspar appears to be mostly orthoclase.	See microphoto. No.9
I	G-19	PIII	Volcanic sandstone	Well sorted, angular to subrounded grains of quartz and sericitized feldspar and andesitic to trachytic rock fragments about 0.5 mm in size are packed in a quartzose matrix. Rouded to subangular opaque mineral grains and epidote are abundantly present.	